



## Advanced Hybrid Engines for Aircraft Development

# AHEAD

### Project Final Report

Project no.:	284636
Instrument:	Collaborative Project (STREP)
Thematic Priority:	FP7, AAT.2011.6.1-2 Propulsion
Start date of project:	1 October 2011
Duration:	39 months
Date of report:	23 /03 /2015
Contact details scientific coordinator	Dr. Arvind Gangoli Rao Associate Professor Propulsion & Power Faculty of Aerospace Engineering Delft University of Technology
	Tel : +31 15 27 83833
	Email: <a href="mailto:A.GangoliRao@tudelft.nl">A.GangoliRao@tudelft.nl</a>

#### Disclaimer:

The information in this document is provided as is and no guarantee or warranty is given that the information is fit for any particular purpose. The user thereof uses the information at its sole risk and liability. The opinions expressed in the document are of the authors only and in no way reflect the European Commission's opinions.

## Table of Contents

Executive Summary .....	3
Summary description of project context and objectives .....	4
Main Scientific Results.....	9
Multi-fuel Aircraft Conceptual Design .....	10
Hybrid Engine Architecture and Performance .....	13
Hybrid Engine Sizing and Weight Estimation.....	17
Hydrogen Combustor .....	20
Flameless Combustor .....	24
Contrail Formation .....	27
Climate Assessment.....	30
Cost Benefit Analysis .....	33
Potential Impact .....	35
Address of project public website and contact details .....	40

CONFIDENTIAL

---

## Final Publishable Summary

### Executive Summary

Aviation is the backbone of our modern society, connecting markets and people worldwide. As in the past, passenger demand and freight traffic is expected to grow at a rate of 5% per year in the next decades. As a result of continuous growth there is concern over the environmental impact of aviation. Today air transport contributes around 3-5 % to Global Warming. In order to reduce the environmental impact despite the increasing future demand, the Advisory Council for Aviation Research and Innovation in Europe (ACARE) has put forth ambitious goals for civil aviation in 2050: CO<sub>2</sub> emissions per passenger kilometre needs to be reduced by 75%, NO<sub>x</sub> emissions by 90% and perceived noise by 65%, relative to the year 2000. Moreover due to the dwindling petroleum reserves, the availability of kerosene cannot be guaranteed in the future.

The AHEAD project proposes a Multi-Fuel Blended Wing Body (MFBWB) aircraft with Hybrid Engines as the next generation aircraft and propulsion system. This novel configuration is a step change in both aircraft design as well as the propulsion system and has the potential to meet the abovementioned future challenges which will be faced by aviation. The MFBWB aircraft carries two kinds of fuel, a clean cryogenic fuel such as Liquid Hydrogen (LH<sub>2</sub>) or Liquid Natural Gas (LNG) and a liquid fuel such as biofuel or kerosene. Cryogenic fuels have a higher energy density compared to kerosene which reduces the total weight of fuel required for the mission however storing these cryogenic fuels is difficult due to their large volume and low temperature requirements. However the proposed MFBWB aircraft overcomes this problem and the hybrid engine enables the optimum usage of these fuels while reducing the overall emissions from the engines significantly.

A conceptual design of the MFBWB aircraft was carried out to see the feasibility of carrying multi-fuels in the aircraft. Several elements of the proposed novel hybrid engine were investigated in the project like the hybrid engine architecture, the hydrogen combustion chamber, the flameless combustion chamber, the overall engine design, engine layout and sizing, etc. The overall impact of the new aircraft and the engine on the climate with respect to global warming (including contrail formation) was looked into.

The results from the AHEAD project suggests that the CO<sub>2</sub> emission from the MFBWB aircraft using LNG and Kerosene is more than 50% less when compared to Boeing 777-200 LR for the same mission. The NO<sub>x</sub>, soot and CO emission can be reduced by more than 80% when compared to the baseline B777-200 ER aircraft. Significant noise reduction is also expected from this novel aircraft configuration due to its embedded aircraft-engine integration.

The AHEAD project paves the way for design of the next generation aircraft and engine technologies which will enhance the efficiency of civil aviation while reducing its environmental footprint.

## Project Context and Objective

### 1.1.1. Motivation: Challenges Faced by Aviation

Aviation is a great contributor to society, bringing people and cultures together and creating economic development across the globe. Air routes are the highways of the global economy. The temporary halt of aviation activities within Europe caused by the volcanic eruptions in Iceland highlighted the deep impact which aviation has on the economy of developed countries. Whereas aviation is vital for the development of economy, there are specific challenges that have to be overcome in order to sustain the future growth of aviation. **Figure 1.1** shows the main challenges faced by aviation today. If the growth in aviation is to be sustained in the future, then these challenges must be addressed soon.

Aviation mainly contributes to the global warming due to CO<sub>2</sub> and NO<sub>x</sub> emissions and due to changes in cirrus cloudiness. The NO<sub>x</sub> predominates both in the vicinity of the airport and also during the cruise. For a long flight, the NO<sub>x</sub> forms a large fraction of the total emissions. The emission norms will become more stringent in the coming years, with the consequent need to reduce pollutants level drastically. The anticipated reduction at various fronts (noise, air pollution and fuel consumption) required to meet the future challenges, as envisioned by the Advisory Committee for Research in Aeronautics (ACARE) is shown in **Fig.1.2**. It is targeted that CO<sub>2</sub> emission has to be reduced by 75%, NO<sub>x</sub> emission by 90% and the perceived noise levels be reduced by 65% when compared to the baseline year 2000. This is to be achieved by a combined improvement in the aircraft, powerplant and the air traffic management system.

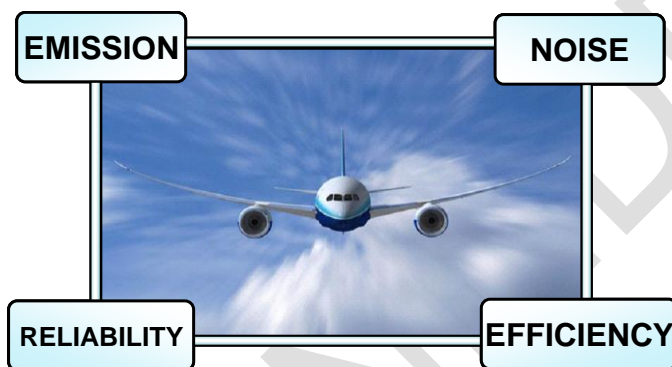


*Fig. 1.1 Main challenges for commercial aviation*

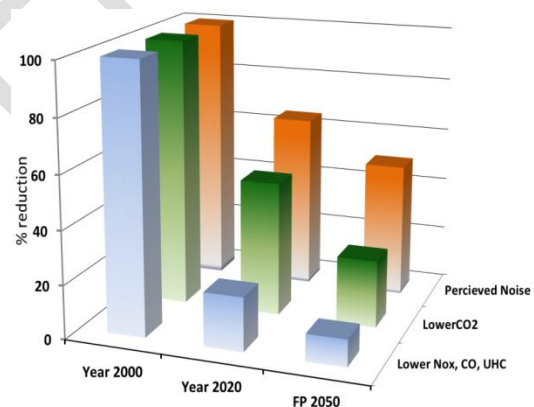


*Fig. 1.2 ACARE vision for Europe*

### 1.1.2. The Multi-fuel Blended Wing Body

As petroleum reserves are depleting, future aviation will encounter a significant use of cryogenic fuels, like liquefied natural gas (LNG) or liquid hydrogen (LH<sub>2</sub>). The energy density of hydrogen is much higher than kerosene, allowing much less fuel to be carried on-board. However, the volume required by hydrogen is much higher than that for kerosene. There are several benefits of using cryogenic fuel on the environment. Several EU sponsored research projects are looking into the production of cryogenic fuel like **GreenAir**, the **FCH JTI**. The EU sponsored project **ALFA-BIRD** has looked into the development of alternative fuels and biofuels for aviation.

The **Cryoplane** concept that was investigated under the 5th Framework Program of the European Commission showed the advantages of using hydrogen for aviation. However the main problem was storing the cryogenic fuel tanks within the aircraft. In a conventional aircraft, fuel is stored in the wings; however cryogenic fuels cannot be stored in the wings because it has to be stored in pressurized cylinders and the wings of a conventional passenger aircraft are too thin to accommodate cylindrical tanks. The LH2 storage scheme envisaged in the *Cryoplane* project is shown below in **Fig. 1.3**. However this configuration is not so suitable from a passenger comfort, safety and aircraft aerodynamic efficiency point of view.

The Multi-Fuel BWB aircraft with the hybrid engine proposed in the AHEAD project is shown in **Fig. 1.4**. It can be seen that the fuel tanks can be stored without interference with the passenger section. The wings of a BWB have sufficient room for storing LH2 tanks. Further away from the centerline where wing thickness is reduced, liquid biofuel can be stored, as shown in **Fig.8**. Thus, a combination of Biofuel and cryogenic fuel seems to be a viable energy source for future aircraft configurations.

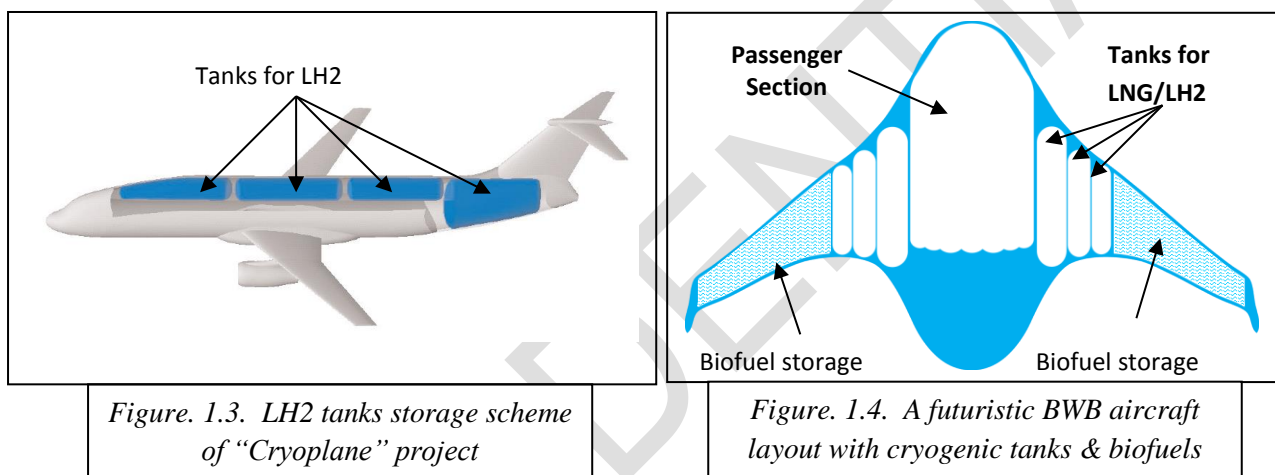


*Figure. 1.3. LH2 tanks storage scheme of "Cryoplane" project*

*Figure. 1.4. A futuristic BWB aircraft layout with cryogenic tanks & biofuels*

The blended wing body configuration seems to be the most promising concept for replacing the current cylindrical centre body fuselage aircraft, which has not changed much since the 1950's. The blended wing body (BWB) has been investigated by many research groups in the world and seems to be the next logical revolution in aircraft configuration. **In fact in a latest statement report, NASA has claimed that the BWB aircraft would be the only solution for future aviation.**

### 1.1.3. Future Engine Requirements

The requirements from an engine for futuristic Multi-fuel blended wing body aircraft are envisioned as follows;

- **Multiple Fuels:** The propulsion system for the Multi-Fuel BWB should be able to burn two fuels in varying quantities depending upon the aircraft requirements while producing low amount of emissions at the same time.
- **Low Emissions:** The target reductions in CO<sub>2</sub>, NO<sub>x</sub> & CO by ACARE in the future have already been shown in **Fig. 1.2**. Reductions in soot emissions are also considered since they affect contrail cirrus properties.
- **Low Noise:** It is targeted that the cumulative noise from engine and airframe should be reduced by 65%, as shown in **Fig.1.2**. Studies have shown that rear, embedded engines are favoured for their potential noise reduction and compatibility with the airframe. However

current turbofans and future ultra-high bypass turbofans are not compatible for this as they cannot sustain the non-uniformities within the flow.

- **Lower Installation Penalty:** The current trend in the gas turbine engines is to increase the engine BPR, which makes them bigger and larger. Even though the Specific Fuel Consumption (SFC) of such engines is lower, the resulting aerodynamic drag and weight is large, thus increasing their installation penalty. The proposed engine for MF-BWB aircraft should be able to reduce the installation penalties when compared to future ultra-high bypass turbofans.
- **Boundary Layer Ingestion (BLI):** Future aircraft designs would have different requirements for the engines in terms of the aircraft-engine integration. The potential advantages of BLI are
  - ❖ Reduces the aerodynamic drag of the aircraft
  - ❖ Increases the propulsive efficiency of the engines
  - ❖ Enables embedded engine installation which can reduce the noise significantly

#### 1.1.4. Novel Features of the Hybrid Engine

In order to meet stringent demands of future aero engines for BWB aircraft, a novel engine configuration has been conceived. The proposed engine is capable of meeting all the requirements mentioned earlier. A schematic drawing of the new engine is shown in Fig.1.4.

#### Novel Features of the Hybrid Engines

- Multiple fuel capability (LH2 and biofuel)
- Dual Combustion chamber (LH2 Combustor & Biofuel / Kerosene Flameless combustor)
- Counter rotating shrouded fans for enhanced propulsive efficiency and Boundary layer ingestion
- Lower engine diameter
- Turbine bleed air cooling by LH2
- Low installation penalty

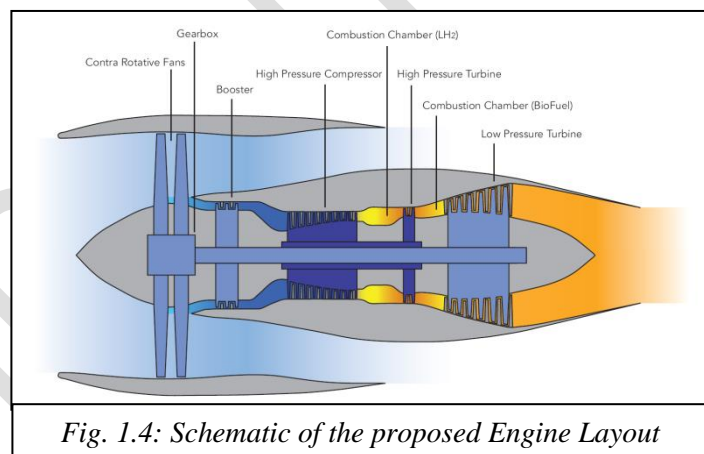


*Fig. 1.4: Schematic of the proposed Engine Layout*

As can be seen, the novel engine proposed is quite different than a conventional turbofan and includes many breakthrough technologies. The various novel technologies involved in the proposed engine configuration.

#### 1.1.5. Objectives

The main objective of the AHEAD project is to evaluate the feasibility of the novel Multi-fuel Blended wing body aircraft and the hybrid engine. The sub objective can be summarized as

- Perform the conceptual design of the MFBWB aircraft and assess its feasibility with respect to CO<sub>2</sub> emission reduction.
- Redefine the paradigms in aircraft propulsion; the project aims to develop a novel propulsion system for the MFBWB aircraft.
- To assess the feasibility and perform an in-depth analysis of the proposed hybrid engine concept.
- To design a suitable hydrogen burner concept for aero engines and prove its feasibility on an experimental test rig.
- To design and test a flameless combustion chamber at atmospheric pressures.

- To further the state of the art in various technologies like next generation engine architecture, hydrogen combustion, low NOx flameless combustion with liquid fuel, bleed cooling, boundary layer ingestion, climate prediction models, etc.
- Evaluate the effect of the new aircraft and engine on the environment and assess its impact on the climate.

CONFIDENTIAL

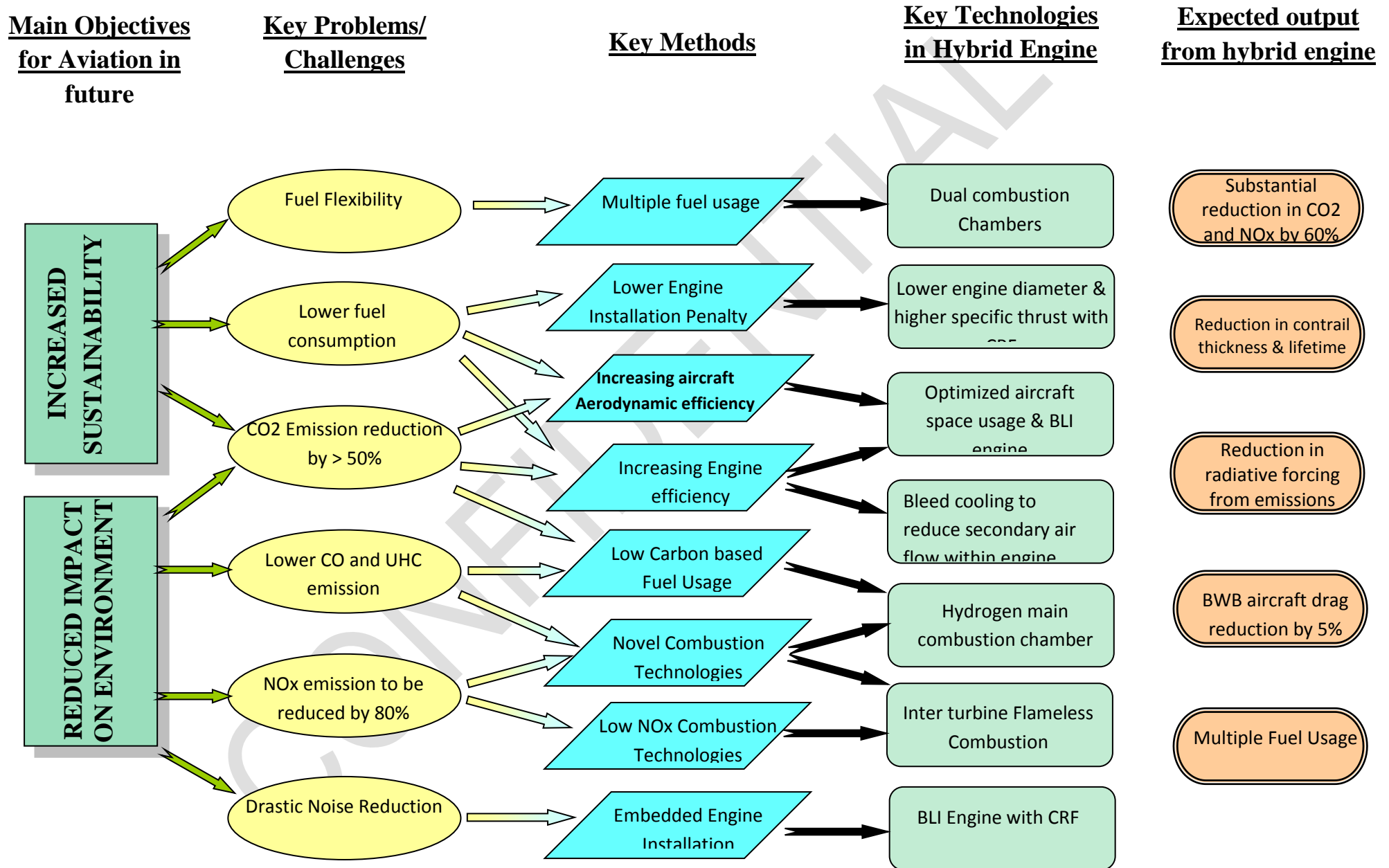


Fig. . The Design Philosophy of the proposed Hybrid Engine



**Main Scientific Results**

The main scientific results have been distributed over according to the various work packages and modules within the WPs

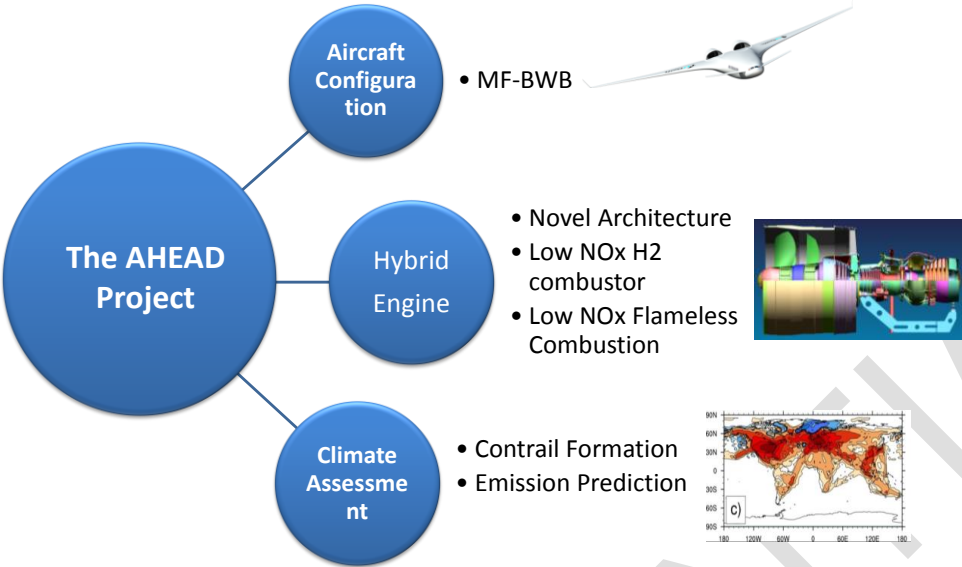


Figure 1: Technologies addressed in the AHEAD project

CONFIDENTIAL

### 2.1. Multi-fuel Aircraft Conceptual Design

The mission requirements for designing the proposed MFBWB aircraft were as follows.

- The BWB aircraft should be multi-fuel (LNG and kerosene)
- The aircraft should carry 300 passengers
- Range of 14,000 km
- Available for 2050

The main reason for choosing this mission is because it is anticipated that this market segment (point to point) will grow more in the wide body aircraft. For the present study, the Boeing 777-200LR was chosen as the baseline aircraft as it fulfills the same mission requirements for year 2000 and therefore can be used for comparing the emissions reductions as set by ACARE. The proposed multi-fuel BWB aircraft is a new kind of aircraft and there exists no prior design for such aircraft. After several iterations, the layout selected for the proposed MF-BWB is shown in Fig. 2.1.1.

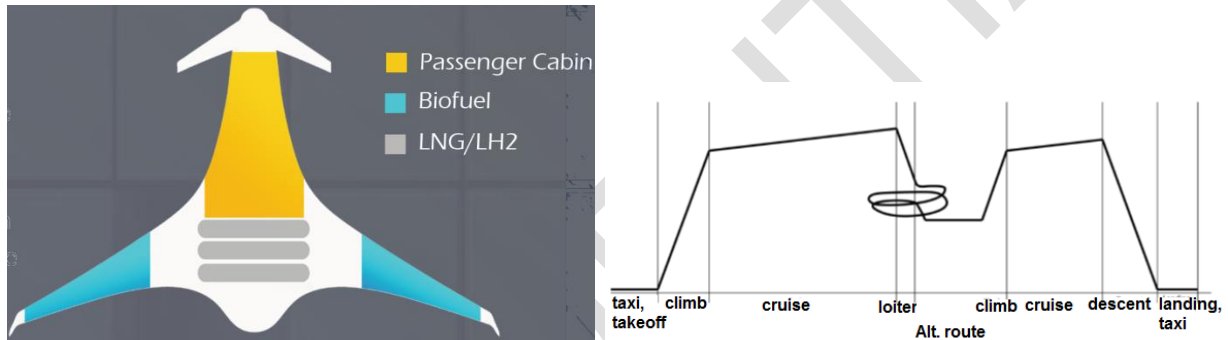


Fig. 2.1.1. Schematic layout for proposed Multi-fuel Blended Wing Body and the mission

The prominent reasons for selecting the layout shown above were passenger evacuation, separation between passenger cabin and cryogenic fuel storage and lower CG variation. To be able to estimate the fuel weight fraction ( $W_f / W_0$ ), the fuel fractions for each flight phase are to be estimated. These flight phases are determined by the mission profile, which is quite a standard profile for an airliner. The fuel fractions are determined by use of statistical values except those for fuel intensive flight phases, namely cruise, loiter and the alternative destination cruise and loiter. The wing loading and the thrust loading are shown in Fig. 2.1.2.

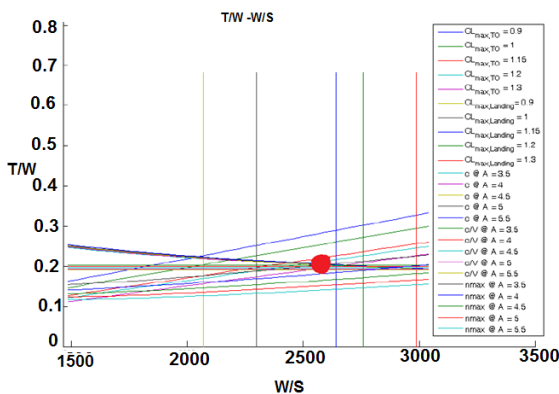


Fig. 2.1.2: The wing loading Vs thrust loading for the MF BWB aircraft.

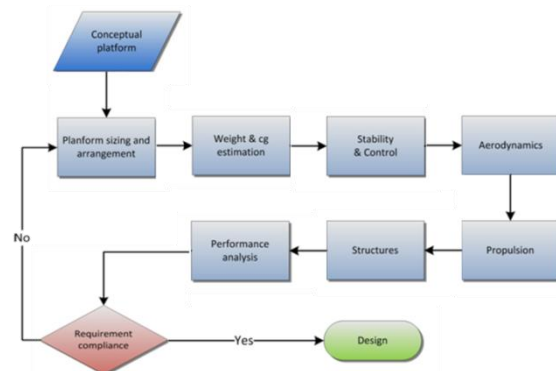


Fig. 2.1.3: The design procedure

An iterative procedure is used as shown in Fig. 2.1.3. The tool consists of a number of modules, each covering their own subjects. The modules are called successively, thus securing a consistent iteration and they use input values obtained from previous modules. Each module creates output values, which are again passed to the next module. For the modules to be used, as well as the order of running them, a procedure, similar to the one described by Roskam part II, is adopted.

The drag divergence curve is approximated as shown in Fig. 2.1.4 (a). The L/D variation of the MF-BWB aircraft is shown in Fig. 2.1.4(b).

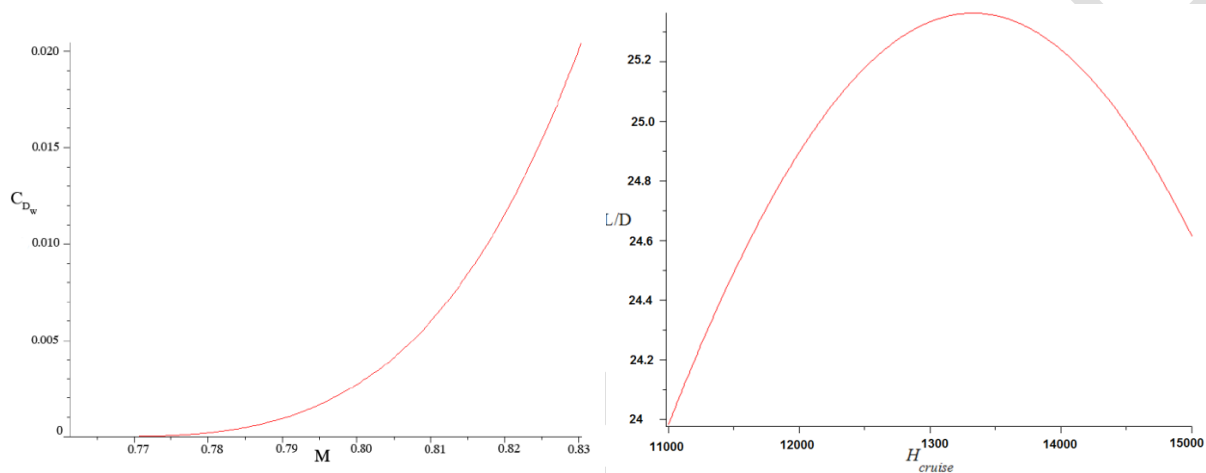


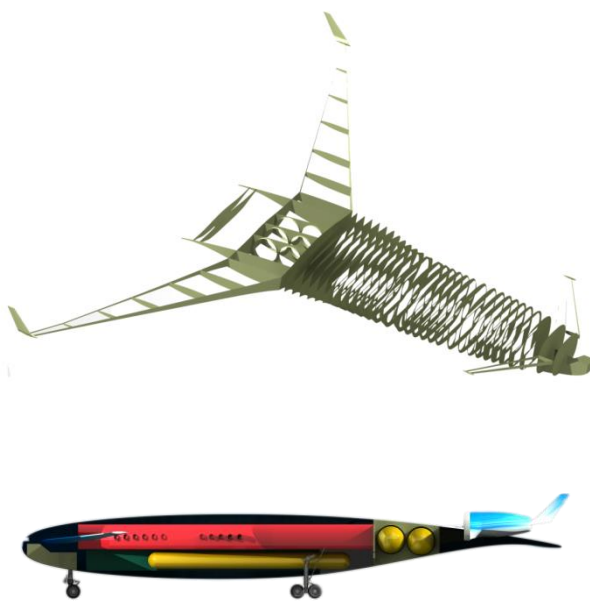
Fig. 2.1.4(a). Estimated wave drag (b) The variation of cruise lift to drag ratio with altitude.

The LNG is stored in cryogenic insulated pressure vessels. The fuel must be stored at lower than 120K. But even when in well insulated vessels some LNG will boil off and evaporate as natural gas. Generally, this boil off gas is removed from the pressure vessel. The boil off gas can be used by the APU or refrigerated back to the liquid state and returned to the pressure vessel.

For designing the tanks, the methodology described by Colozza<sup>1</sup> is used. The cryogenic pressure vessels are assumed to be made from carbon fiber reinforced polymer. The ultimate tensile strength of the used pre-impregnated carbon fiber is 1250 MPa. A factor of safety of 2.5 is used in the design.

The volume needed to store the LNG is approximately 124m<sup>3</sup>. This volume is divided over 4 pressure vessels. Two of the pressure vessels are located alongside the cargo compartment in longitudinal direction. The other two are located after the passenger and cargo compartment in lateral direction. The two pressure vessels alongside the cargo compartment have the same dimensions. These tanks have a length of 17.4m and a radius of 0.7m. The other two pressure vessels are placed behind the passenger cabin (across the length of the aircraft), and have a length of 10.3m and a radius of 1.15m. The placement of the tanks is shown in Fig. 2.1.5. The internal aircraft structure is also shown in the same figure.

<sup>1</sup> Colozza, A.J., "Hydrogen Storage for aircraft Applications Overview", NASA/CR-2002-211867.



	MF-BWB
Wo	242,800 kg
MTOW	237,970 kg
OEW	122,220 kg
W/S	265.04
(T/W)TO	0.21
TTO	527,810 N
Tcruise	98,195 N

Fig.2.1.5. Placement of LNG tanks in the aircraft and the main weight parameters.

The comparison of the layout of the BWB to the Boeing 777-200ER is provided in 2.1.6. The shorter and wider body of the aircraft makes it aerodynamically more efficient than a conventional cylindrical body aircraft. Combined with the advanced hybrid engine, the multi-fuel BWB is able to reduce CO<sub>2</sub> emission by around 60% than a conventional Boeing 777-200ER aircraft.

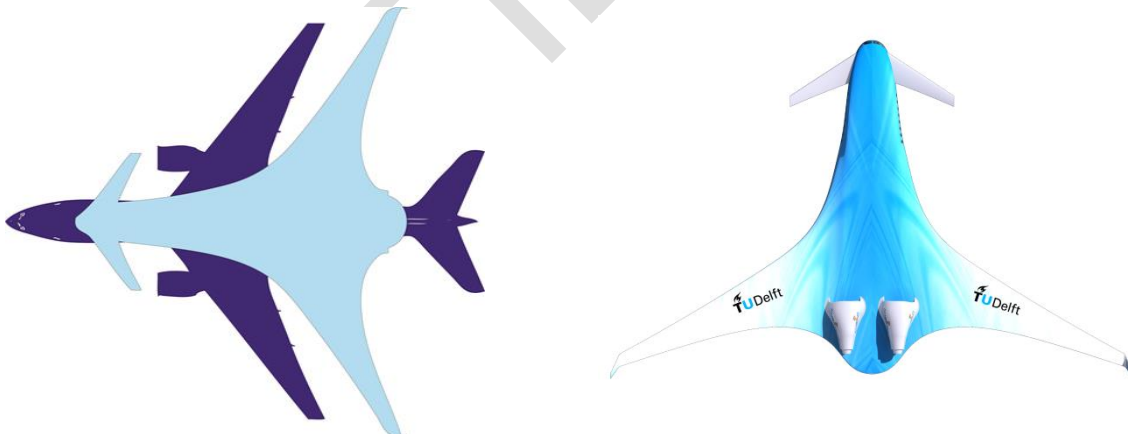
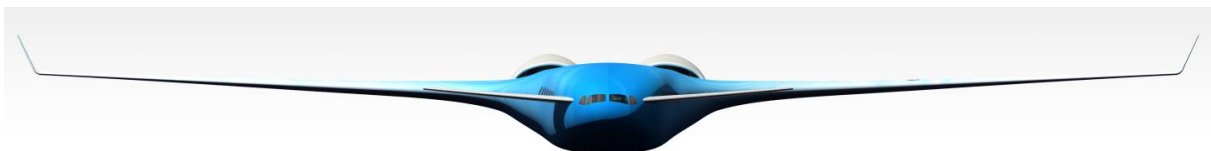


Fig. 2.1.6. Comparison of the MF-BWB layout with the Boeing777-200ER.



## 2.2. Hybrid Engine Architecture and Performance

To exploit the unique opportunity provided by the above mentioned multi-fuel BWB aircraft, a novel multi-fuel hybrid engine concept integrating all the requirements described in the previous session has been conceived. The salient features of this engine are:

- **The Hybrid Dual Combustion System:** The proposed innovative hybrid engine uses two combustion chambers as shown in 2.2.1. The main combustor operates on LH2 while the second combustor (ITB, between HPT and LPT) uses biofuel or kerosene in the flameless combustion mode. Such a novel combustion system has never been used before for aero engines and provides several advantages like low NO<sub>x</sub>, fuel flexibility and better off-design performance.
- **Bleed Air Cooling:** The cryogenic fuel used in the main combustion chamber is an excellent heat sink and can be used for cooling the bleed air prior to combustion via a heat exchanger, thus reducing the amount of bleed air required substantially. Also by using this novel technique, the amount of heat released by the cryogenic fuel in the combustion chamber increases slightly, thereby decreasing the amount of fuel required in the combustion chamber.
- **Contra Rotating Fan:** The proposed hybrid engine with counter rotating fans will have a smaller diameter and higher propulsive efficiency for the same bypass ratio. Also since each stage of the fan is less loaded as compared to single stage fan architecture, a Contra Rotating Fan (CRF) can sustain more non uniformities in the flow generated due to BLI as compared to a conventional architecture.

Four engine architectures listed below incorporating partially or fully the features described above were evaluated.

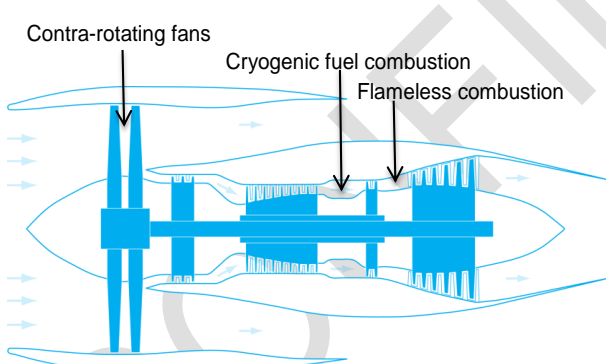


Figure 2.2.1: The Schematic of the basic unmixed hybrid engine concept

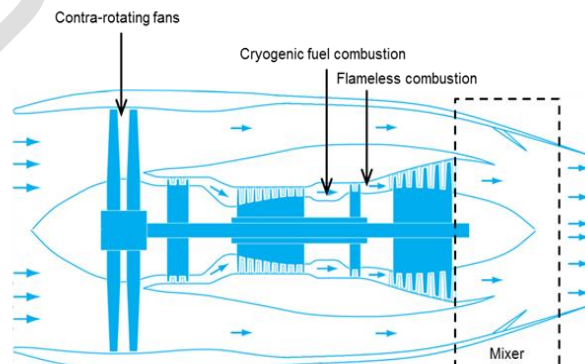


Figure 2.2.2: The Schematic of the basic mixed hybrid engine concept

- a) Concept in a) with an additional bleed air cooling system in 2.2.3

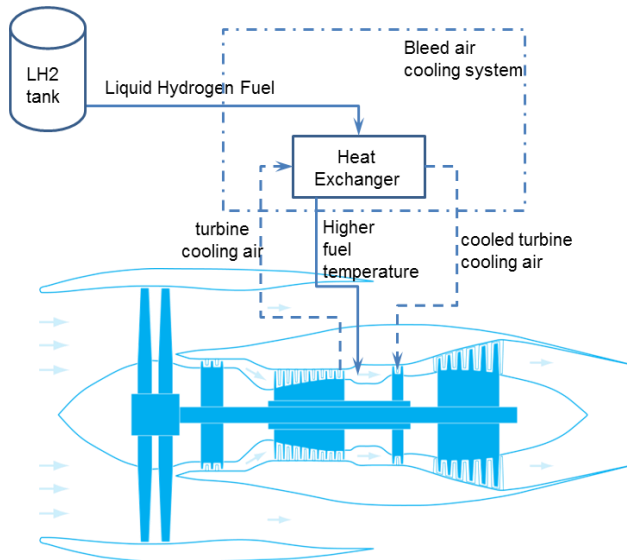


Figure 2.2.3: The Schematic of the engine concept a) with a bleed air cooling system

**Parametric analysis of the selected hybrid engine configuration**

To analyse the parametric characteristics of the hybrid engine, a 0-D thermodynamic model is created. Gas turbine Simulation Programme (GSP) was selected as a modelling tool. Component-based gas turbine modelling environment of GSP (GSP-Development-Team, 2010) provides the flexibility to model various gas turbines, especially those having novel architectures, for instance, the hybrid engine. The model is validated with GE90-94B engine.

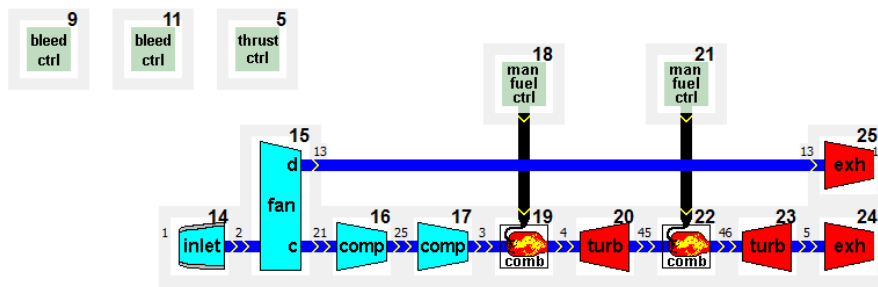


Figure 2.2.4: The layout of a hybrid engine model in GSP.

**Parametric analysis**

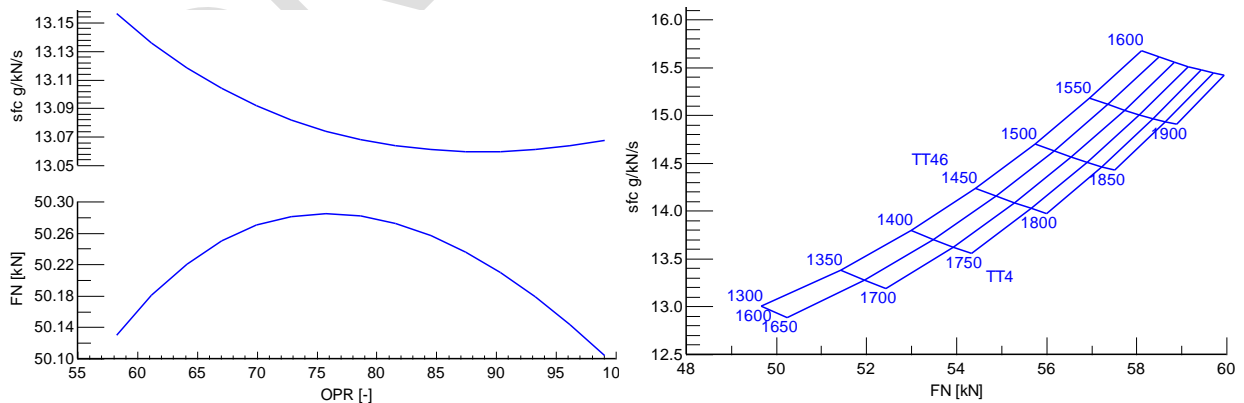


Figure 2.2.5: The variation of SFC and FN various design parameters.

## Performance optimization at a cycle reference point

There are several numerical optimization algorithms. For the engine cycle optimization, a non-gradient based optimization methods using genetic algorithm was chosen. Genetic algorithm can deal with a variety of problems whether the objective function is linear or nonlinear, stationary or non-stationary, continuous or discontinuous. The GSP model is coupled with the with the genetic algorithm for engine optimization is presented. Proper population size, number of generations, rate of crossover or mutation, and selection criteria were selected based on the results obtained from the sensitivity analysis results.

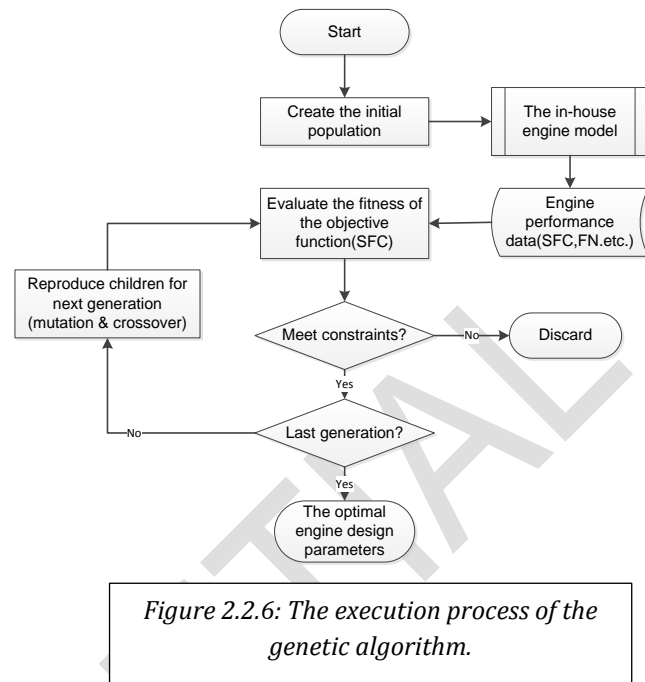


Table 2.1.1 Optimized engine design parameters and performance.

LH2 & Kerosene		LNG & Kerosene	
Design Parameters		Design Parameters	
BPR	15	BPR	15
FPR	1.5	FPR	1.5
LPC pressure ratio	3.9	LPC pressure ratio	3.9
HPC pressure ratio	11.2	HPC pressure ratio	11.2
Tt4, K	1600	Tt4, K	1600
Tt46, K	1315	Tt46, K	1441
Engine Performance		Engine Performance	
SFC, g/kN/s	13.2	SFC, g/kN/s	14.3
ST, N.s/kg	120.7	ST, N..s/kg	127.6
LH2 energy fraction	0.88	LNG energy fraction	0.75
LH2, kg/s	0.2072	LNG, kg/s	0.4578
Kerosene, kg/s	0.0808	Kerosene, kg/s	0.1819

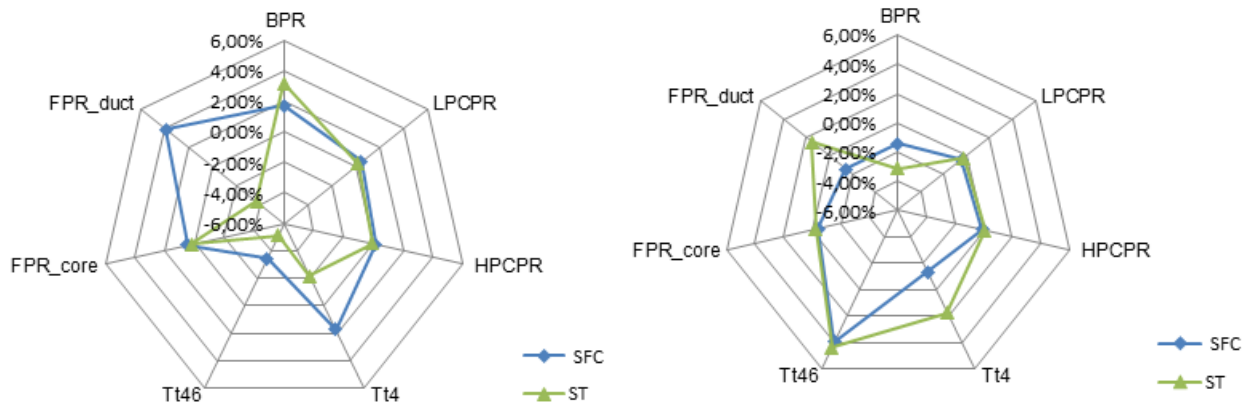


Figure 2.2.7. Variation of SFC, and ST with 5% increment and 5% decrease of design parameters.

### The hybrid engine performance evaluation

The performance of the hybrid engine has been compared to the baseline engine GE90-94B at a reference point. The results are shown in **Error! Reference source not found.** It indicates that the LH2 version hybrid engine can reduce the CO<sub>2</sub> emission by around 94%, and the SFC by 12%. However, the specific thrust is 1% less. On the other hand, for the LNG hybrid engine, CO<sub>2</sub> and the SFC are lowered by 57% and 4% respectively. In contrary to the LH2 engine, the LNG engine can still benefit in ST by 5% more.

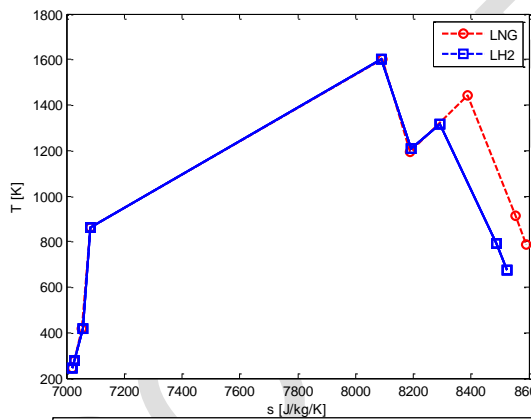


Fig. 2.2.8. The hybrid engine T-s diagram for LNG and LH2.

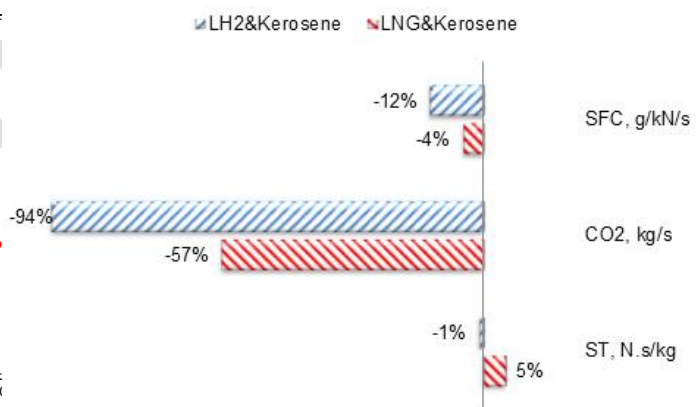


Fig.2.2.9. Comparison of the hybrid engine to GE90-94B



### 2.3. Hybrid Engine Sizing and Weight Estimation

The Hybrid engine sizing was defined based on engine architecture similar to PW4000 engine in the same class trust as AHEAD engine with required updated and scaling to match hybrid engine requirements. XXI century engines development trends and technology were implemented to be as close as possible to the latest engines models state-of-the-art technology. The CRF version, due to the lower fan diameter assumed, can be competitive to the other types of the engine, as the engine drag is lower. The CRF engine diameter is output of fan blades design and gearbox speed ratio possibilities to optimize LTP efficiency. Fan Blades material has been replaced to composites, while in previous version it was titanium. Composites are most advanced materials used for Fan Blades and will continue to be developed in the future. Due to lower density and acceptable durability a weight reduction of almost 200 kg was achieved in the Fan module.

The weight of both engines was estimated based on 3D models with applied materials considered for those parts design. For CRF engine weight was calculated for two versions, depended on Gearbox:

- for Gearbox with Double Planetary System total weight is 7257 kg
- for Gearbox with Differential System total weight is 7224 kg.

The rest of parts in those two CRF options are the same, the difference is limited to Gearbox. The weight analysis results (with double planetary system and with differential system) hybrid engine versions is shown on further figures and diagrams.

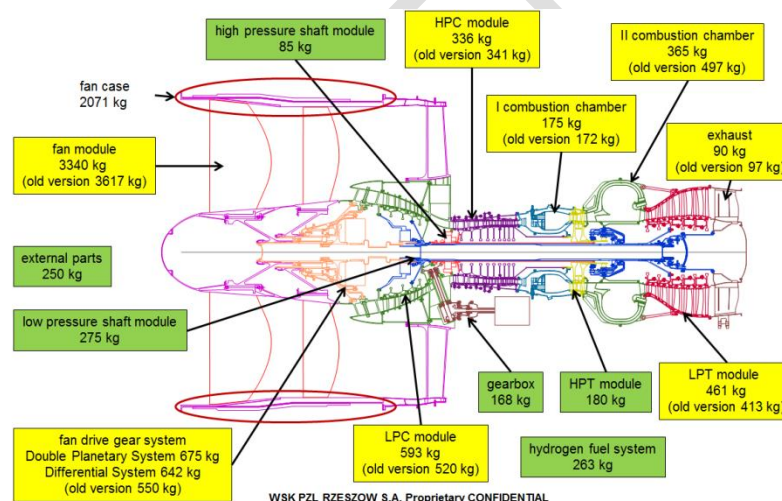


Fig 2.3.1. AHEAD hybrid CRF engine modules final configuration weight summary with indication of changes (yellow highlights for optimized design changes).

The CRF engine weight comparison includes both gearbox versions developed and optimized. The design provided in AHEAD project for the double planetary gearbox is reasonable solution for the fan stages requirements and speed settings. Engine weight of the double planetary system is only 33kg higher than initial differential version. The CRF gearbox weight is similar to GTF gearbox, which relatively higher weight comes from the single stage integration and mechanical constraints. Major weight contributors for CRF versions were highlighted on Fig.2.3.2. All changes related to modules were clarified and weight difference highlighted. Cases, supporting structures, combustors items can still participate in weight drop as design can be further optimized in the subsequent follow on program. Significant weight decrease is the matter of future materials and design approach and manufacturing methods development.

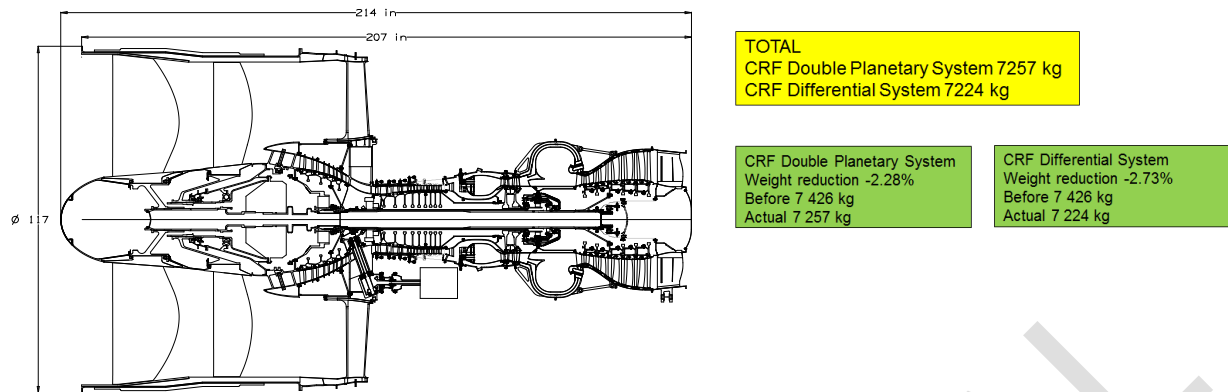


Figure 2.3.2. AHEAD hybrid CRF engine final dimensions and weight.

Comparing AHEAD CRF Engine with Differential System and the same class trust PW4164, the weight of AHEAD CRF final configuration is 1373 kg higher, which is 23% more. Engine diameter is almost the same,  $\phi 123$  inches - PW4156 and  $\phi 127$  inches - AHEAD CRF version. Total length of AHEAD CRF engine is 20 inches longer with compared PW4156 (187 inches versus 167 inches in PW4156). Those numbers shows that adding second fan with gearbox as well as Flameless Combustor to the existing engines results with increased weight for AHEAD CRF engine version.

3D model of the engine was defined for reference and for hybrid engine development. 3D model of the hybrid engine was defined covering design intention from developed 2-D layout with specific 3D design implementation related to the gearbox. Based on design requirements and criteria for mechanical constraints and engine turbomachinery loads, the geometry of various parts were defined and validated with analytical tools and shown as representative 3D model. Based on 3D engine model, the dimensional and weight analysis was provided. Heat Exchangers (HEX) locations are a matter of the maintainability and certification aspects. HEX's can be a part of the aircraft fuel supply and evaporation system or they can be positioned on the engine like it was initially presented in WP1.3. Weight of hydrogen fuel system was included in the overall engine weight calculation.

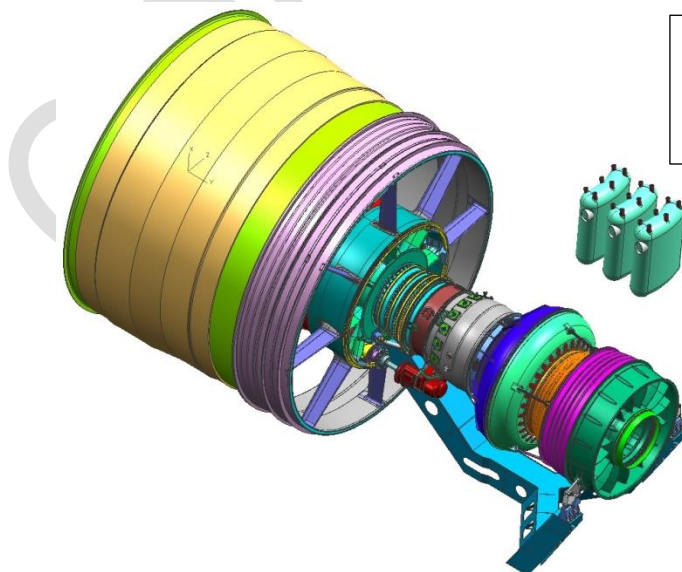


Figure 2.3.3. General isometric view of the AHEAD CRF hybrid engine with Heat Exchangers modules positioned outside engine.

Final optimized design engine concept is shown on Fig. 2.3.4. The hybrid engine core definition with developed concepts of hydrogen and flameless combustor are shown. Final configuration was developed in parallel and with iteration between engine layout definition and combustors design development from task 2.5. The main challenge was flameless combustor structural design and its incorporation within the hybrid engine as it was not typical for existing engines. The design was evaluated and finally defined to meet assembly and maintainability aspects taking manufacturing considerations into account. The CRF blades concept provided by TUD was described in D1.3 section. As the CRF fan stages can be defined with different settings, both differential and double planetary gearbox was investigated and conceptual design provided as the proof that the engine is promising concept with possibilities for further development.

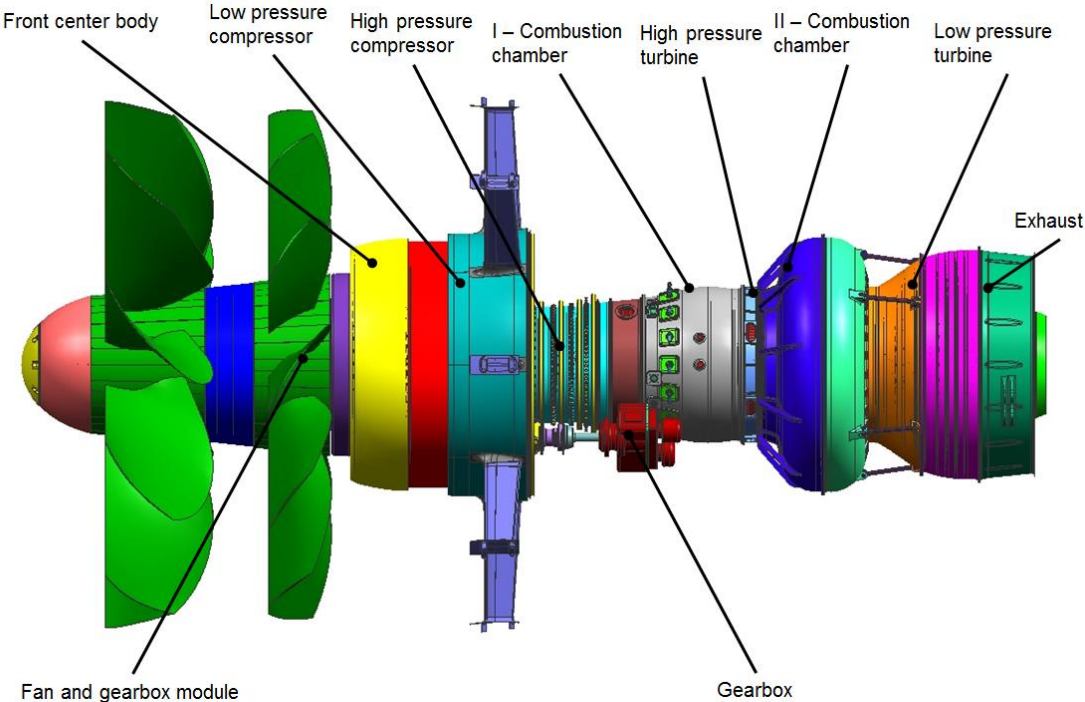


Figure 2.3.4. AHEAD CRF hybrid engine modules review.

COM

## 2.4. Hydrogen Combustor

### Concept

In the current investigation a center body-less mixing tube and lean premixed, swirl stabilized combustion is applied. Such a setup promises very low NO<sub>x</sub> emissions and was successfully applied to other modern combustor concepts<sup>2</sup>. For lean premixed combustion, with increasing fuel reactivity, the lean blow out limits are extended but flashback disposition is increased<sup>3</sup>. The burning velocity of hydrogen is one order of magnitude greater in comparison to methane<sup>4</sup>, making hydrogen flames prone to flashback. Common measures against flashback are increase in bulk air velocity or decrease in swirl intensity. These measures come with a significant trade-off in terms of increased pressure loss and degraded fuel air-mixing (Reichel et al. 2013)<sup>5</sup>, respectively. While increased pressure loss reduces the engine efficiency, decreased fuel air-mixing quality increases NO<sub>x</sub> emissions. Another approach with little trade-off is to inject an air film to lean out the wall-near boundary layer, which is particularly susceptible to flame propagation, due its low velocity level<sup>6</sup>. This approach is successfully used in the current setup to suppress wall boundary layer flashback.

As a measure to suppress flashback, the proposed burner applies axial air injection on the central axis of the radial swirl generator. It is applied with the intention to create a plug flow-like axial velocity profile at the nozzle exit and shift the stagnation point downstream. This technique vastly extends the operational range with pure hydrogen. With a high amount of axial air injection, flashback is suppressed for the entire operational range of the atmospheric test rig (compare **Error! Reference source not found.**). At the same time, single digit NO<sub>x</sub> emissions up to adiabatic flame temperatures of  $T_{ad} = 2000\text{K}$  could be maintained (Reichel et al. 2014)<sup>7</sup>.

### Hydrogen Burner Concept

**Error! Reference source not found.** provides a schematic of the investigated swirl burner. There are two ways for the main air flow to enter the cylindrical mixing tube (red). First, through the radial swirl generator (green), whereby a certain amount of swirl is imposed on the flow, depending on the number of blocking rings (blue). Second, through an orifice of the diameter  $D_{or}$  on the central axis (yellow), constituting the axial air injection.

The amount of axially injected air is not metered but adjusted only by the ratio of pressure loss between the swirl generator and axial injection orifice. Therefore, varying the orifice diameter  $D_{or}$  allows to adjust the axial volume flow  $\dot{V}_{ax}$ . The fuel is injected into the premixing section through sixteen injection ports located on an annular ring around the truncated center body. The mixing tube is located downstream of the swirl generator and has an inner diameter of  $D =$

<sup>2</sup> Döbbling, Klaus; Hellat, Jaan (2007): 25 Years of BBC/ABB/Alstom Lean Premix Combustion Technologies. In: *Journal of Engineering for Gas Turbines and Power* 129 (1), S. 2–12.

<sup>3</sup> Schefer, R.W; Wicksall, D.M; Agrawal, A.K (2002): Combustion of hydrogen-enriched methane in a lean premixed swirl-stabilized burner. In: *Proceedings of the Combustion Institute* 29 (1), S. 843–851.

<sup>4</sup> ILBAS, M.; CRAYFORD, A.; YILMAZ, I.; BOWEN, P.; Syred, N. (2006): Laminar-burning velocities of hydrogen-air and hydrogen-methane-air mixtures: An experimental study. In: *International Journal of Hydrogen Energy* 31 (12), S. 1768–1779.

<sup>5</sup> Thoralf G. Reichel; Steffen Terhaar; Christian O. Paschereit (2013): Flow Field Manipulation by Axial Air Injection to Achieve Flashback Resistance and its Impact on Mixing Quality. In: 43rd Fluid Dynamics Conference: American Institute of Aeronautics and Astronautics (Fluid Dynamics and Co-located Conferences).

<sup>6</sup> Burmberger, Stephan; Sattelmayer, Thomas (2011): Optimization of the Aerodynamic Flame Stabilization for Fuel Flexible Gas Turbine Premix Burners. In: *Journal of Engineering for Gas Turbines and Power* 133 (10).

<sup>7</sup> Reichel, Thoralf; Terhaar, Steffen; Paschereit, Christian Oliver (2014): Increasing Flashback Resistance in Lean Premixed Swirl-Stabilized Hydrogen Combustion by Axial Air Injection. In: *Journal of Engineering for Gas Turbines and Power*.

34mm. Auto ignition has been considered in the design process and the residence times in the premixing section are designed to remain below the autoignition delay times.

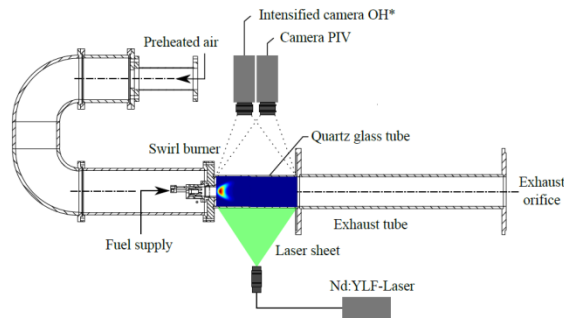


Figure 2-4-2: Experimental setup for simultaneous PIV and OH\* measurements in atmospheric combustion test rig

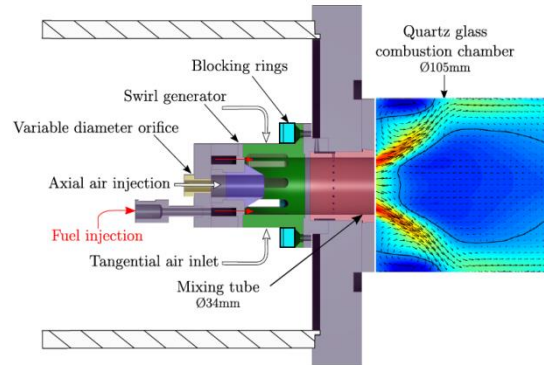


Figure 2-4-2: Schematic of burner model, indicating different volume flow pathways through swirl generator or axial injection

Since strong acceleration of the flow, appearing in converging nozzles, prevents a relocation of the flame in the combustion chamber in case of flashback, a cylindrical shape of the mixing tube was chosen. For the water tunnel experiments a Plexiglas model of the burner was designed that, in addition to the combustion chamber, also provided full optical access to the mixing tube.

## Results

The isothermal tests were carried out to measure the velocity field in both, mixing tube and combustion chamber. The aim is to prove that axial air injection alters the flow field in a manner desired for increased flashback resistance.

### Isothermal Velocity Field

The velocity field inside the mixing tube and the combustion chamber is investigated in a water tunnel in order to assess the impact of axial injection. Characteristics of the flow field in the absence and presence of a medium ( $D_{or} = 8.0\text{mm}$ ) and high amount ( $D_{or} = 8.8\text{mm}$ ) of axial air injection for a swirl number of  $S = 0.9$  are presented in Figure 2.4. For all investigated conditions, vortex breakdown is established downstream of the area expansion. This leads to the typical flow field of swirl-stabilized combustors, which constitutes in an inner recirculation zone (IRZ), enveloped by an annular jet, and an outer recirculation zone (ORZ) between the annular jet and the bounding walls.

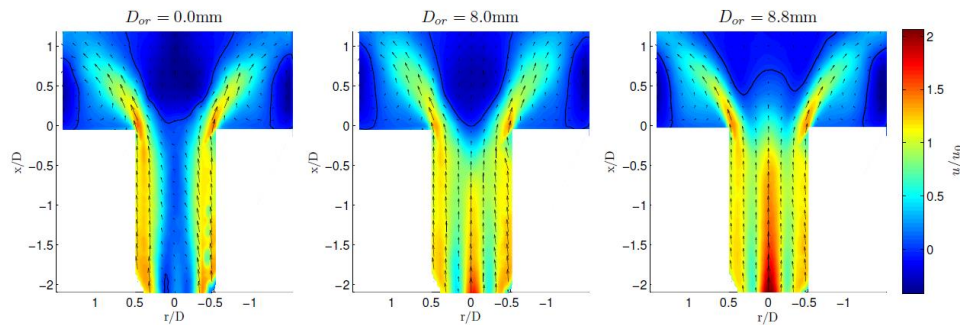


Figure 2.4.3: Velocity vectors superimposed on normalized mean axial velocity of the isothermal flow field in the absence ( $D_{or} = 0\text{mm}$ ) and presence of a medium ( $D_{or} = 8.0\text{mm}$ ) and high ( $D_{or} = 8.8\text{mm}$ ) amount of axial air injection (long mixing tube;  $S = 0.9$ ), solid lines.

### Evaluating Mixing Properties by Laser Induced Fluorescence

The introduction of a non-swirling jet on the central axis of the premixing section could be suspected to degrade the fuel-air mixing. Therefore, the fuel-air mixing in the presence of axial air injection was investigated in a water tunnel. It was found, that spatial unmixedness is slightly increased, whereas temporal unmixedness gets even decreased. In summary, fuel-air mixing remains excellent and, thus, also emissions are expected to remain very low.

### Operational Limits and Stability Map

Reacting tests at the atmospheric combustion test rig of the HFI, revealed that the concept of axial air injection allows for flashback-proof swirl-stabilized combustion of technically premixed hydrogen mixtures. Note, that at least a medium amount of axial injection was mandatory to operate the burner with undiluted hydrogen. In the presence of a high amount of axial air injection, no occurrence of flashback was observed at the investigated conditions, namely inlet temperatures up to 700K at stoichiometric conditions and combustor power from 20-220 kW. In case of a medium rate of axial air injection, flashback was observed when decreasing the equivalence ratio. However, all configurations could operate at stoichiometric conditions. This observation contradicts the increase of flame speed with equivalence ratio, but can be explained by the hydrogen, due to its associated high volume flow, changing the flow field (please refer to (Reichel et al.) for further details).

### Emissions

The NO<sub>x</sub> concentration for the hydrogen combustion plotted with respect to the calculated adiabatic flame temperature is presented in Figure 0. The emissions of configuration 4 are very low and remain below 13 ppm (dry at 15% O<sub>2</sub>) up to a calculated adiabatic flame temperature of  $T_b = 2000\text{K}$  up to inlet temperatures of 700 K. For a high amount of axial air injection and swirl number  $S = 0.9$ , the burner's emissions remain below 10 ppm (dry at 15% O<sub>2</sub>) and also below emissions of the case with a medium amount of axial injection. It is, thus, proven that the concept of axial air injection allows to increase flashback safety and extend the operational range while at the same time decreasing NO<sub>x</sub> emissions.

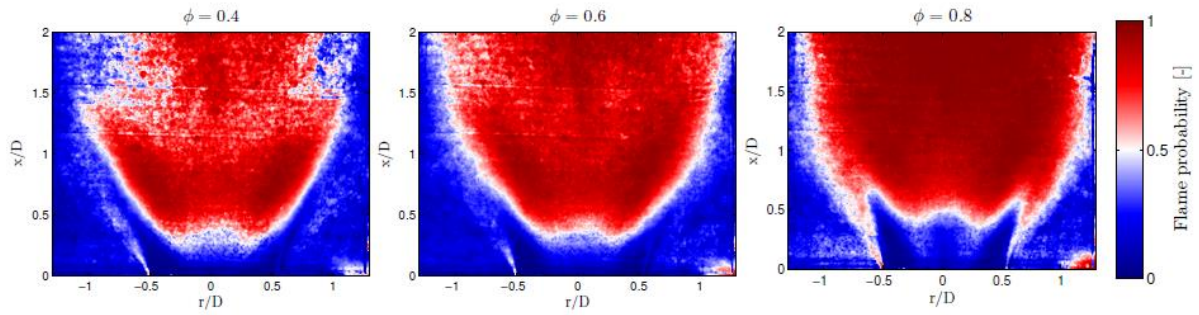


Figure 0: Flame probability indicating the likelihood of the flame to appear in a certain region, hence, allowing to determine the upstream flame shape ( $Re = 75000$ ).

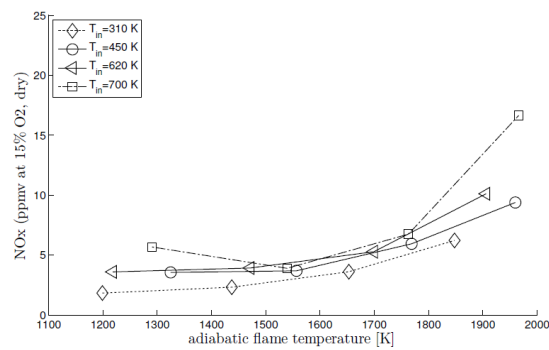


Figure 0:  $NO_x$  emissions (dry) plotted over the calculated adiabatic flame temperature for configuration 4 at increasing inlet temperatures  $T_{in}$ .

## 2.5. Flameless Combustor

The 2nd (sequential) combustor operates under vitiated conditions, namely, the incoming oxidant is air that already participated in the combustion process within the 1<sup>st</sup>, hydrogen fuelled combustor. Due to the lean hydrogen combustion conditions, its exhaust gases include oxygen in sufficient concentration to allow a 2<sup>nd</sup> stage combustion process downstream of the engine's high pressure turbine stage. Due to the high temperature of the incoming oxidant stream ( $T=1201\text{K}$  for cruise and  $1300\text{L}$  for Take-Off) and its low oxygen concentration (17.3%), the novel and low NO<sub>x</sub> flameless oxidation mode of combustion was selected. The challenge was to design and test a combustor which could operate in the flameless combustion regime in a stable way while producing low emissions and complying with certain dimensional limitations within the engine. The design space for 2nd combustor compartment may be relatively large and includes the cavity between the shaft and the fan duct as can be seen in Figure 2.5.1. This large cavity is typically not used for any specific needs and can be used for the flameless combustor. An optimal configuration was selected that complied with the requirements of both, cruise and take-off conditions. A separate task was performed to validate the ability of the CFD code to model accurately the combustion process within the flameless combustor which has two distinct characteristics: 1.) it is fed with high inlet temperature vitiated air and, 2.) the combustor process should result in relative low temperature rise which require very low global equivalence ratio. The current best configuration is described in Fig. 2.5.2 which also shows the main flow streams and the fuel injection points.



Figure 2.5.1: Space allocated for the combustor

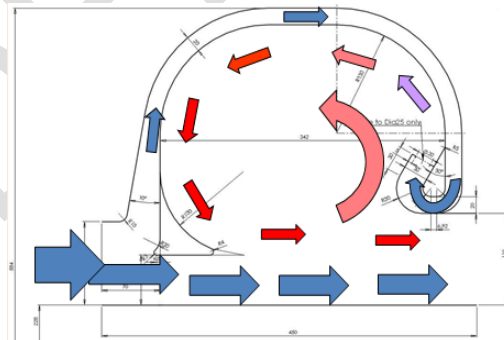


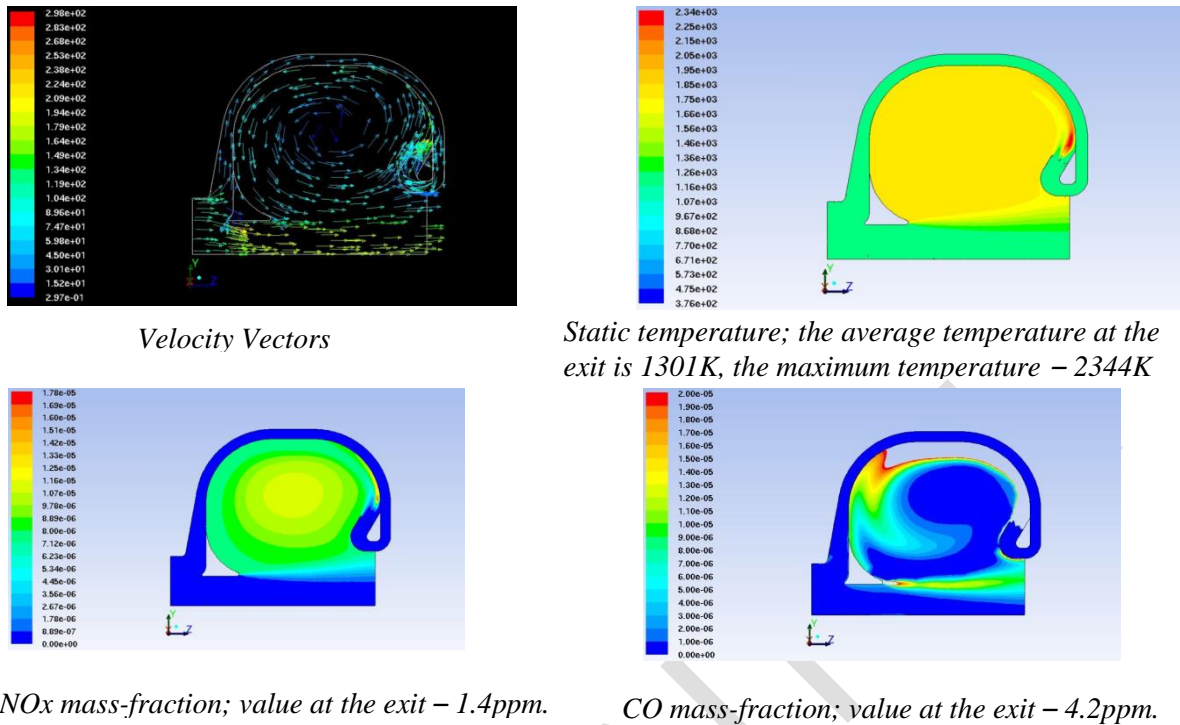
Figure 2.5.2: Schematic of the secondary flameless combustor.

Using the chemical kinetics and CFD simulations, the AHEAD's Secondary combustor was able to demonstrate the desirable performance for cruise and take-off conditions. A selection of charts from the detailed description of the result, are shown in Fig. 2.5.3. The design described in Fig. 2.5.2 resulted in CO emission of 4.2 ppm and NO<sub>x</sub> emission of 1.4 ppm with total pressure drop equal to 2.4%, see table 1 and Fig 2.5.3.

Table 2.5.1: Simulations of emissions during Cruise and Takeoff, best results.

Condition	NO <sub>x</sub> , ppm	CO, ppm	$\Delta P$ , %	UHC, ppm	Comments
Cruise	8.6	2.4	2.4	0.00006	RUN 42, kerosene, vapor
Cruise	0.5	14.4	2.4	2.0	RUN 54, kerosene, 120°, spray
Take Off	13.2	0.7	3.5	0.002	RUN 28, kerosene, vapour, rough mesh





Static temperature; the average temperature at the exit is 1301K, the maximum temperature – 2344K

NOx mass-fraction; value at the exit – 1.4ppm.

CO mass-fraction; value at the exit – 4.2ppm.

Figure 2.5.3: The distribution of static temperature, velocity vectors and NOx and CO, as calculated by CFD simulations.

As the analysis of the flameless combustor was based mainly on CFD, experimental verification was needed to validate the accuracy of the simulated results and by that, the validity and feasibility of the flameless combustor's design. A scaled down model of the combustor was designed, simulated and tested to confirm the ability of the CFD code to evaluate the combustion performance of the experimental model and by that, also that of the full scale combustor. Scaling down of the geometry was by factor of 3 (linearly) and similarly for the velocities (to maintain equal residence time), resulting in total air mass flow rate of 10 gr/sec.

The detailed description of the CFD simulations and experimental results for the experimental model are given in a separate report, the deliverable D2.4 of the AHEAD program. Figure 2.5.4 show the variation of CO and NOx emissions due to the addition of nitrogen (N2). Adding N2 is an experimental exercise by which one can evaluate the effect of reducing the O2 content in the oxidant in order to learn more about the effect of air vitiation, as in the AHEAD hybrid engine in which a portion of the O2 is consumed and were water vapours are added.

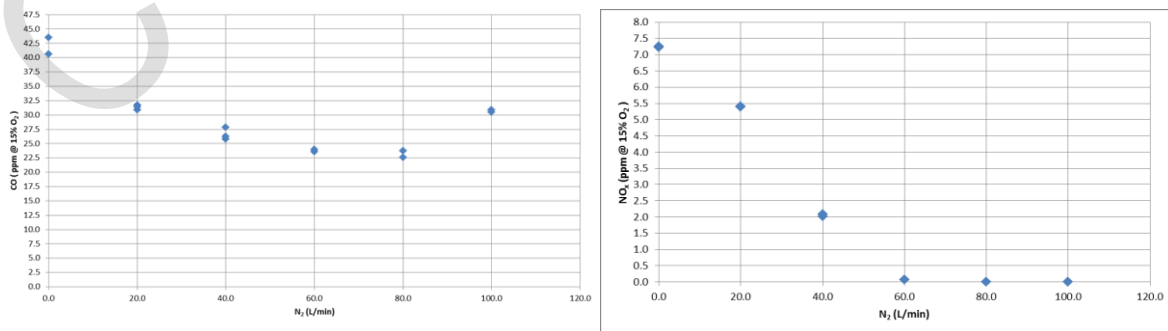


Figure 2.5.4: variation of CO and NOx with nitrogen addition, air flow rate 230 l/min, no water addition, Power: 2.8 kW --  $\phi_{Global}$  : 0.19 -- Air : 230 L/min -- Water: 0 g/h.

The effect of equivalence ratio on emission of CO and NO<sub>x</sub> where the oxidant was pure air can be seen in Fig. 2.5.5. The figures demonstrate the classic chart of CO and NO<sub>x</sub> vs. equivalence ratio however they are “squeezed” towards low values. Typically, the minimum CO value is achieved at higher equivalence ratios whereas here it is at a value of about 0.16. However, this may not seem significantly exceptional considering the fact that similarly to a classical jet engine combustor, here as well, one may consider that in the flameless combustor there is also a combustion zone and a dilution region and hence the local equivalence ratio within the combustion zone is significantly higher than the global equivalence ratio. As for the NO<sub>x</sub>, one can see the monotonic increase of NO<sub>x</sub> with equivalence ratio, however, the specific reason for the reduction of NO<sub>x</sub> at high equivalence ratios, has to be further investigated.

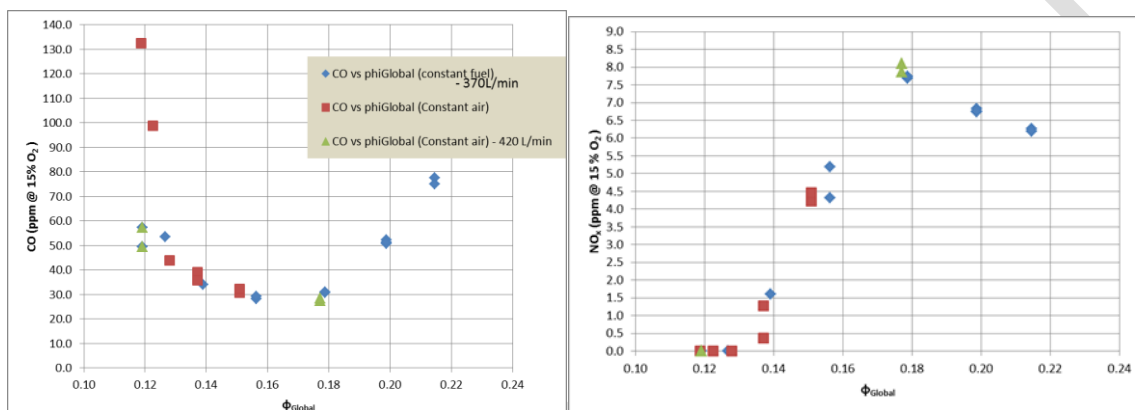


Figure 2.5.5: Variation of CO and NO<sub>x</sub> with  $\Phi_{global}$ , air flow rate 230 l/min, no water or nitrogen addition. Constant Fuel: Power: 3.3

## Discussion and Conclusions

The combustor’s design was performed using different chemical kinetic mechanisms of kerosene combustion and CFD simulations. The best results achieved for cruise conditions for CO and NO<sub>x</sub> emissions were obtained where fuel was introduced in the form of liquid spray: 14.4 ppm for CO and 0.5 ppm for NO<sub>x</sub> with pressure drop equal to 2.4%.

Condition	NO <sub>x</sub> , ppm	CO, ppm	$\Delta P$ , %	UHC, ppm	Comments
Cruise	8.6	2.4	2.4	0.00006	RUN 42, kerosene, vapor
Cruise	0.5	14.4	2.4	2.0	RUN 54, kerosene, 120 degs. spray
Take Off	13.2	0.7	3.5	0.002	RUN 28, kerosene, vapour, rough mesh

Table 2.5.2 Cruise and Takeoff simulations, best results

The main simulated results show that for cruise and takeoff, the aerodynamics within the combustor is characterized by a large recirculation region which is a key requirement for achieving flameless condition. Due to the fact that the obtained experimental results exhibited similar behavior as the CFD simulations, we conclude that the CFD tool with the applied turbulence and combustion models is suitable to evaluate the combustor performance. To conclude, the combustor design suggested herewith can perform according to the hybrid engine requirements. As a final note, the current study has highlighted the potential of the flameless combustion in aircraft engines.

## 2.6. Contrail Formation

The climate impact of contrail cirrus has been shown to be the largest air traffic related forcing component when using current aircraft (Burkhardt and Kärcher, 2011)<sup>8</sup>. A change in the formation probability when switching to LH2 or LNG technology could therefore have a large impact on the overall climate impact due to air traffic. Contrails can form when during mixing of the hot and moist exhaust with the cool and dry environment the air becomes saturated and water droplets can form, which then freeze. This formation process depends on the slope,  $G$ , of the mixing trajectory between exhaust and ambient air.

$$G = \frac{c_p \cdot p}{\varepsilon} \cdot \frac{EI_{H_2O}}{(1 - \eta) \cdot Q}$$

In table 2.6.1 we present for both AHEAD engine concepts the water vapor emission index,  $EI_{H_2O}$ , the fuel heat value,  $Q$ , and the overall propulsion efficiency,  $\eta$ . These quantities have been computed using engine design specifications. For comparison we also compute the factor  $g$  (which is the factor  $G$ , taken in Pa/K, divided by the ambient pressure  $p$ , taken in hPa, so that  $g$  consists only of aircraft and fuel specific quantities), i.e.

$$g := \frac{G/p}{\left(\frac{Pa}{K}\right)/hPa}$$

For the conventional kerosene aircraft, assuming similar  $\eta$  as for the AHEAD ones,  $g=7.74 \cdot 10^{-3}$ . Thus the mixing trajectory for an AHEAD engine is at least 2.45 (LH2) or 1.52 (LNG) times as steep as the one of a present day conventional aircraft. The probability for contrail formation of an AHEAD aircraft is much larger and contrails and persistent contrails can form in warmer ambient conditions compared to kerosene driven conventional aircraft as long as temperatures are below about  $-38^\circ\text{C}$ , the temperature at which droplets freeze and form ice crystals. This means that for AHEAD engines contrails can form also at lower flight altitudes. In the tropics this difference in threshold formation temperature is of great importance since the formation probability is increased particularly at the main flight levels. In the extratropics the probability is increased at levels with little air traffic.

version	$EI_{H_2O}$ (kg/kg)	$Q$ (MJ/kg)	$\eta$	$g$
LH2	7.21	101.2	0.396	$1.91 \cdot 10^{-2}$
LNG	2.15	49.3	0.389	$1.17 \cdot 10^{-2}$

Table 2.6.1: Characteristic figures determining the slope of the mixing trajectory,  $G$ , in the Schmidt-Appleman criterion for the LH2 and LNG versions of the AHEAD engine designs.

Aircraft emissions do not only change the formation criteria for contrail formation but also have an effect on the ice crystal number concentrations within the contrails. A newly developed contrail cirrus parameterization was applied to estimate the impact of reduced soot particle number emissions on contrail properties. The new parameterization includes a 2-moment-microphysical scheme simulating contrail mass and contrail ice crystal number concentrations. This allows the estimation of the mean ice crystal radius and therefore a more realistic simulation of sedimentation and optical properties of contrails. The reduction of particle emissions that is thought to cause a decrease in initial contrail ice particle number is expected to change contrail cirrus microphysical processes and may be leading to a reduction of the contrail

<sup>8</sup> Burkhardt, U. & Kärcher, B., "Global Radiative Forcing from Contrail Cirrus", Nature Climate Change, Vol. 1, pp54-58, 2011.

cirrus life time and optical depth, both leading to a decrease in the climate impact of contrail cirrus.

Using this model we estimate the climate impact of contrail cirrus for the AHEAD LNG and LH2 aircraft. We compare the basic scenario, a simulation of the B787 at flight level 390, with the two AHEAD aircraft at flight level 430. Therefore we substitute 50 percent of the flight emissions in FL 370 and FL 380 in the global AERO2k inventory with the respective aircraft emissions at the given flight level.

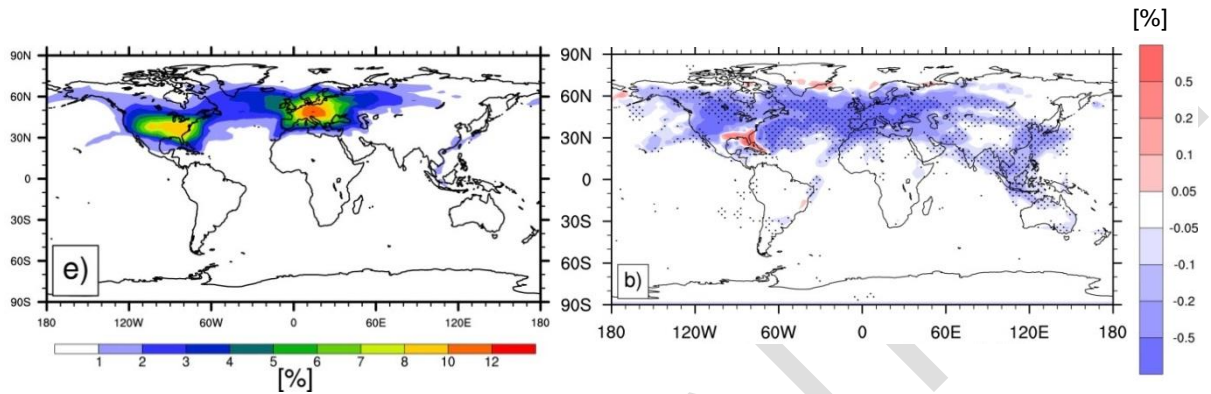


Figure 2.6.1: Total visible coverage (left) in scenario with AHEAD-LNG at flight level 430 and changes (right) compared to basic scenario, shaded regions are significant.

The visible coverage of contrail cirrus with optical depth greater than 0.02 in the simulation of AHEAD-LNG at flight level 430 is significantly reduced in the main flight corridors when compared to the basic scenario (B787 at FL 390), (Fig. 2.6.1). In the extra tropics coverage is decreased since the aircraft at the higher flight altitude already flies in the dry stratosphere. In the tropics we shift air traffic into the upper troposphere where the formation conditions for contrails are better, because in the tropics at FL 390 it is usually the temperature criterion that prohibits contrail formation. At FL 430 contrail formation conditions are the same for all aircraft considered since temperatures are very low. The reduction of the initial ice particle number due to reduced soot emissions results in a decreased optical depth of contrail cirrus dominating the change in radiative forcing. The global pattern of radiative forcing remains the same (Fig.2.6.2).

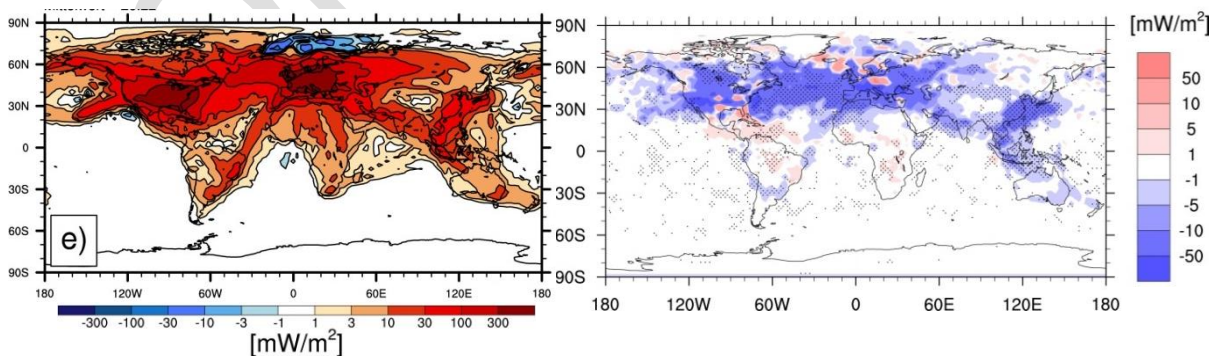


Figure 2.6.2: Radiative forcing (left) in scenario with AHEAD-LNG in FL 430 and changes (right) compared to basic scenario, shaded regions are significant.

Globally the reduction in radiative forcing is 10 (7) percent for the AHEAD-LNG (AHEAD-LH2) aircraft as compared to the B787 at the lower FL 390 and 7 (4) percent for the AHEAD-LNG (AHEAD-LH2) aircraft as compared to the B787 at the same FL 430 (Tab.2.6.2). All differences of

global values are not significant because the small perturbation we include in the climate model compared to the natural climate variability would require a very large number of simulated years. Nevertheless, the local significance especially in the main flight regions shows us that the recent estimates are plausible.

For LNG driven aircraft the change in the formation probability is smaller than for the LH2 fuelled aircraft. Changes in contrail cirrus coverage and radiative forcing are very similar to changes for LH2 planes but slightly smaller.

	Changes relative to B787 (FL 390)	Changes relative to B787 (FL 430)
AHEAD LNG	0.90	0.93
AHEAD LH2	0.93	0.96

*Table 2.6.2: Factor for reduced radiative forcing of contrail cirrus in simulations with AHEAD aircraft compared to simulations with B787.*

CONFIDENTIAL

### 2.7. Climate Assessment

The climate impact of air traffic results from CO<sub>2</sub> emissions and non-CO<sub>2</sub> effects, such as contrails, changes ozone and methane due to NO<sub>x</sub> emissions, water vapour and particles. Each aircraft and mission has a different characteristic and hence climate impact. Hence a careful consideration of the regarded scenario and climate assessment is necessary. AHEAD regards the reduction of the long-term climate impact of a fleet of AHEAD aircraft with an entry into service by 2050 and reaching a certain market share by 2075, compared to a reference fleet with a conventional future technology. This guarantees a fair comparison at the same technology level and the same route network.

Five aircraft are compared. As a today’s reference a B787-8 aircraft is regarded. For a future conventional reference a B787-8 is taken including some future expected enhancements, such as an increased propulsion efficiency and bio fuel (called “B787-FUT”), following ideas of Flightpath2020. As a comparison to this reference also “B777-200ER” is taken into account. These aircraft are then compared to an AHEAD aircraft, which is either fuelled with LNG and bio fuel or LH2 and bio fuel. Since LH2 has a low density the required storage might lead to a larger aircraft with increased weight, a minimum and maximum weight AHEAD-LH2 aircraft is considered.

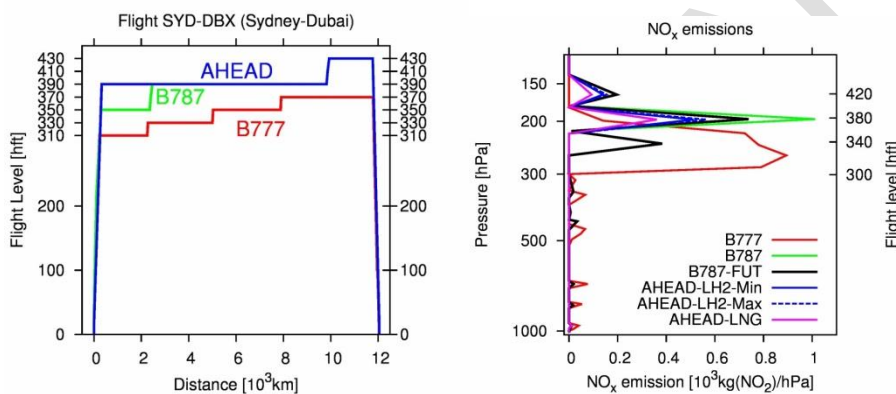


Fig. 2.7.1. Left: Flight profiles for the route Sydney to Dubai; Right: Annual global mean emission profile for nitrogen oxides.

As a route network major cities and long-range international flights are analysed with standard flight profiles (Fig. 2.7.1, left). Generally, the B787 and AHEAD aircraft have higher flight altitudes compared to B777, which has an impact on the effect of non-CO<sub>2</sub> emissions (Fig. 2.7.1, right), especially NO<sub>x</sub> and water vapour emissions. The total calculated annual mean emissions of the AHEAD aircraft are around 50 to 70% smaller than the future reference B787-FUT (Tab. 2.7.1). Other emissions, contrail formation and contrail characteristics differ also significantly. Carbon dioxide and nitrogen oxide emissions are much smaller for the AHEAD aircraft, but water vapour emissions are larger than for the conventional technology B787-FUT.

	B787-FUT	AHEAD-LH2-Min	AHEAD-LH2-Min	AHEAD-LNG
CO <sub>2</sub> [Tg/year]	6.2	1.9	2.1	6.2
H <sub>2</sub> O [Tg/year]	3.3	7.0	7.7	4.7
NO <sub>x</sub> [Gg(NO <sub>2</sub> )/year]	31	13	14	9

Tab. 2.7.1: Global and annual emissions of the reference and AHEAD aircraft (2075).

From the flight profiles and the total emission rates it is clear that opposing effects occur. The lower NO<sub>x</sub> and CO<sub>2</sub> emissions of the AHEAD aircraft will lead to a smaller climate impact than the reference aircraft. However, the larger H<sub>2</sub>O emissions at high cruise altitudes lead to a larger climate impact. Hence the climate impact of the AHEAD aircraft is more driven by water vapour and contrails compared to the reference aircraft, where the climate impact is driven by CO<sub>2</sub>, NO<sub>x</sub> (O<sub>3</sub>) and contrails (Fig. 2.7.2).

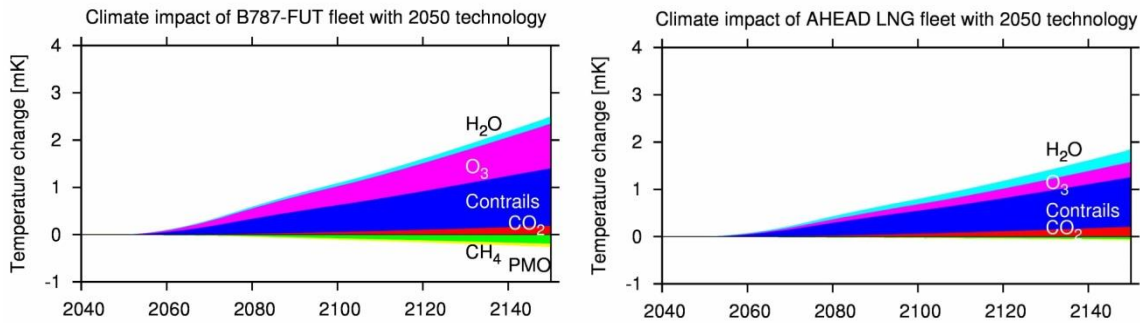


Fig. 2.7.2. Change in global mean near-surface temperature caused by emissions from the B787-FUT (reference) and AHEAD-LNG aircraft.

Clearly the AHEAD fleet emissions lead to a smaller climate impact than a comparable conventional aircraft. A reduction of around 10% of the LH2/bio fuel aircraft is achieved in comparison to the reference conventional aircraft and around 20% for the LNG/bio fuel version (Fig. 2.7.3). The reduction in the NO<sub>x</sub> emissions is driving the reduction in the climate impact. A reduction in the contrail climate impact of around 10% adds to the overall climate impact reduction of the AHEAD aircraft (see Sec. 2.6), resulting from the low particle emissions.

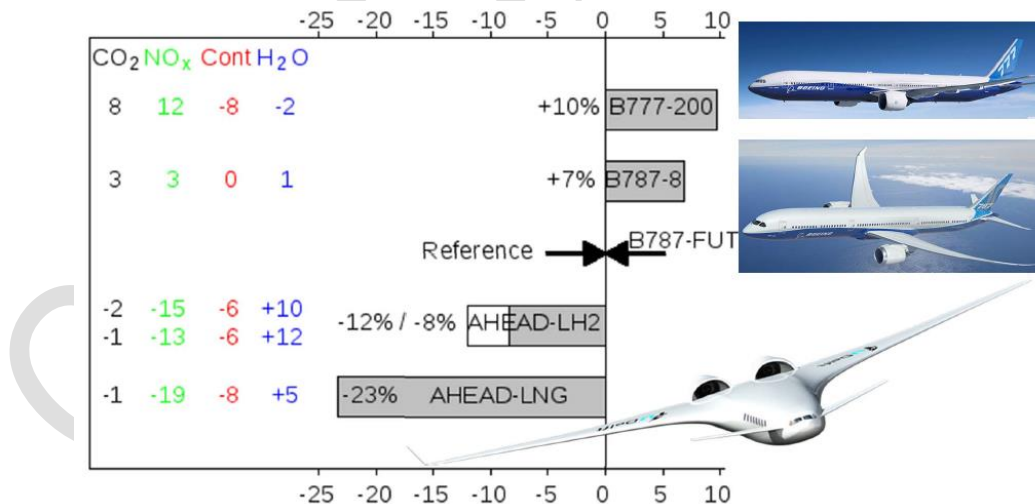


Fig. 2.7.3. Overall climate impact assessment: Relative change in the 100 year-mean future temperature change (%) for the individual aircraft scenarios (identical to relative change in equivalent CO<sub>2</sub> – eqCO<sub>2</sub> emission). B787-FUT is taken as a reference. Total relative changes are shown at the bars, the contribution (%) from different emissions are added on the left. The sum equals the totals, though rounding errors might occur.

The regarded aircraft have different seating capacities. In terms of passenger kilometres the AHEAD fleet has a larger transport volume than the regarded reference fleet. Hence the climate

impact per passenger-km is even more reduced for the AHEAD technology (Fig. 2.7.4). A more than 40% reduction in the climate impact is found for the LNG/bio fuel driven aircraft and a 30% to 35% reduction is found for the B787-FUT reference aircraft.

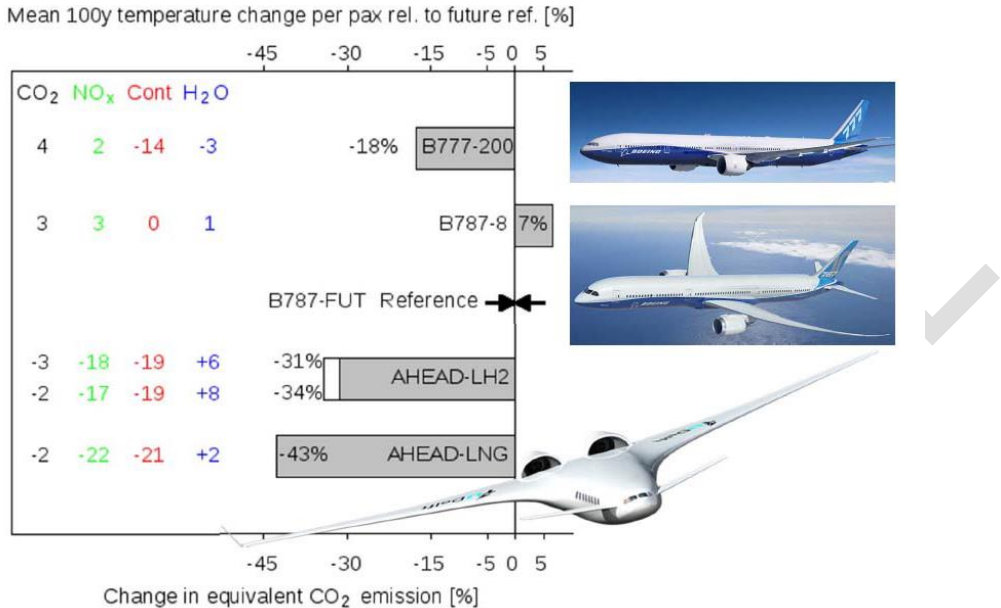


Fig. 2.7.4. As Fig 2.7.3 but relative to the same passenger kilometres.

CONFIDENTIAL



## 2.8. Cost Benefit Analysis

Within the AHEAD project, a detailed cost benefit analysis was carried out. All the major elements which contribute towards the direct operating cost were taken into account. Two routes were selected for the study, Amsterdam (AMS) to Buenos Aires (EZE) and New York (JFK) to Hong Kong (HKG). Cost elements of the Direct Operating Cost like ATM fees, airport charges, flight and cabin crew, insurance are deemed to be the same for each aircraft.

We assumed that the procurement cost of the B777-200 is \$ 296 million (Flight magazine 22-28 April 2014). Of this the 2 engines are cost \$ 32 million. We estimates that the procurement cost of the hybrid engines will be € 40 million. The Ahead multi fuel blended wing body aircraft cost was assumed at € 350 million per aircraft including the new engines and the pressure vessels.

The table below shows the interest rates per flight for the two aircraft.

	<b>B777-200</b>	<b>MF-BWB with hybrid engine</b>
Cost	\$ 296 million	\$ 350 million
Interest/ year 4%	\$ 11.840.000	\$ 14,000,000
Hours per year	14.3 hours per day or 4500 hours per year	14.3 hours per day or 4500 hours per year
Interest per hour	\$ 2,631	\$ 3,111
Interest AMS/EZE	\$ 33,968/ € 26,129	\$42,496/ € 32,689
Interest JFK/HKG	\$ 38,334/ € 29,975	\$47,909/ € 36,853

The table below gives the details of the depreciation for the two aircraft

	<b>B777-200</b>	<b>MF-BWB with hybrid engines</b>
<b>Total cost</b>	\$ 296 million	\$ 350 million
<b>Aircraft</b>	\$ 264 million	\$ 310 million
<b>Depreciation per year</b>	\$ 9,504. 000	\$ 11,160.000
<b>Hours per year</b>	4.500	4500
<b>Depreciation per hour</b>	<b>\$ 2.112</b>	<b>\$ 2,480</b>
<b>Engines</b>	\$ 32 million	\$ 40 million
<b>Depreciation per year</b>	\$1.600.000	\$ 2,000.000
<b>Hours per year</b>	4.500	4500
<b>Depreciation per hour</b>	<b>\$ 356</b>	<b>\$ 444</b>
<b>Total depreciation per hour</b>	<b>\$2.468</b>	<b>\$ 2,924</b>
<b>EZE/AMS</b>	<b>\$ 31.837/ € 24,490</b>	<b>\$ 39,942/ € 30,725</b>
<b>JFK/HKG</b>	<b>\$ 36.403/ € 28,002</b>	<b>\$ 45,030/ € 34,638</b>

The table below gives details of the maintenance cost for two aircraft from EZE/AMS route.

	<b>B777-200</b>	<b>MF-BWB with hybrid engines</b>
<b>C check</b>	1.612,50	\$ 1,088
<b>D check</b>	1.225,50	\$ 680
<b>Engine overhaul</b>	2.580,00	\$ 4,080
<b>Engine LPP</b>	525,00	\$ 520
<b>Landing gear</b>	160,00	\$ 160
<b>Wheels/ brake</b>	480,00	\$ 480
<b>APU</b>	1.419,00	\$ 1,428
<b>Component overhaul</b>	5.289,00	\$ 5,644
<b>total</b>	<b>\$ 13,291</b>	<b>\$ 14,080</b>
	<b>€ 10,224</b>	<b>€ 10,830</b>

**Total fuel cost per flight:****B-777 flights:**

<b>B777</b>	<b>EZE/AMS</b>	<b>JFK/HKG</b>
Fuel	96.710 kg	106.699 kg
Cost/Kg	€ 0,95/kg	€ 0,95/kg
<b>total</b>	<b>€ 91.874,50</b>	<b>€ 101.364,00</b>

Note that even if biofuels were blended with regular petroleum based fuel, the price would not differ.

Total cost for the MF-BWB aircraft with the AHEAD engine

LNG version: it is calculated that the aircraft would use 30% of regular fuel and 70% LNG.

<b>LNG BWB</b>	<b>EZE/AMS</b>	<b>JFK/HKG</b>
<b>Fuel</b>	15.274 kg	16.855 kg
<b>Cost fuel/kg</b>	€ 0,95/kg	€ 0,95/kg
<b>Total</b>	€ 14,510	€ 16,012
<b>LNG</b>	35,639 kg	39,328 kg
<b>LNG/KG</b>	€ 0,77	€ 0,77
<b>Total</b>	€ 27,442	€ 30,282
<b>Total cost</b>	<b>€ 41,952</b>	<b>€ 46,294</b>

Total cost for the MF-BWB aircraft with the AHEAD engine

LH2 version: it is calculated that the aircraft would use 25% of regular fuel and 75% LH2.

<b>LH2 BWB</b>	<b>EZE/AMS</b>	<b>JFK/HKG</b>
<b>Fuel</b>	18,779.9 kg	20,723,8 kg
<b>Cost of fuel/kg</b>	€ 0.95/kg	€0.95/kg
<b>Total</b>	€ 17,841	€ 19,688
<b>LH2</b>	15,629 kg	17,246.8
<b>Cost LH2/kg</b>	€ 3.80 /kg	€ 3.80/kg
<b>Total</b>	€ 59,390	€ 65,538
<b>Total cost</b>	<b>€ 77,231</b>	<b>€ 85,226</b>

<b>Comparison of B777 &amp; MF-BWB with LNG</b>			<b>Comparison of B777 &amp; MF-BWB with LH2</b>		
	<b>CO2 low</b>	<b>CO2 high</b>		<b>CO2 Low</b>	<b>CO2 high</b>
B777	€ 175,932	€ 182,654	B777	€ 175,932	€ 182,654
MF BWB LNG	€ 131,662	€ 134,890	MF BWB LH2	€ 171,981	€ 173,289
Difference	€ 44,270	€ 47,764	Difference	€ 3,951	€ 9,365
CO2 saving	174.7ton	174.7 ton	CO2 saving	270.6 ton	270.6 ton
CO2 saving in %	52%	52%	CO2 saving in %	80%	80%

As can be seen from the table above, the LNG version of the MF-BWB has 25% lower operating costs when compared to B777.

## Potential Impact

As already mentioned in the earlier sections, the AHEAD project investigated the feasibility of powering the future Multi-Fuel Blended Wing Body aircraft (MF-BWB) with hybrid engines, which will be more environmentally friendly than current high bypass ratio turbofan engines used in modern passenger aircraft.

The AHEAD project was a unique project in that sense since it looked at the aircraft and the engine along with the climate assessment. This new level of integration brought experts from various specializations on one platform and gave more insight in the design of integrated aircraft and propulsion solutions for the future air transport scenarios. The project looked at various technologies as shown in the Fig.3.1.

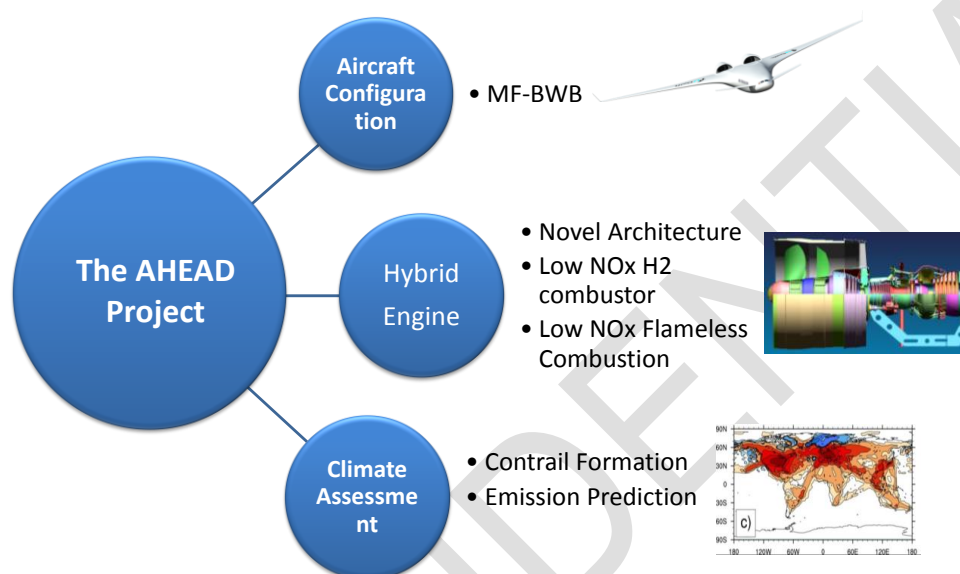


Fig. 3.1 The Novel Technologies that were investigated in the AHEAD project

### 3.1 The Multi-Fuel BWB aircraft

The AHEAD project designed a Multi-fuel Blended Wing Body aircraft in which the large insulated cryogenic fuel tanks for Liquid Hydrogen or Liquid Natural Gas can be accommodated without significant drag penalty. The aircraft was designed by TUDelft and is called a Multi-Fuel Blended Wing Body (MF-BWB) aircraft. The shape of the aircraft is derived from a well-known Blended Wing Body configuration where not only the wings but also the fuselage will create lift making it an aerodynamically attractive aircraft.

The aircraft is unique and offers several advantages with respect to current BWB aircraft designs, the main reasons are as follows

- The MF BWB has smaller passenger capacity as compare to other similar BWBs.
- The proposed configuration is suitable for a family concept, thus the fuselage can be extended and reduced by changing the canard size.
- The MF-BWB is not as wide as other BWBs, making it comfortable from a passenger experience point of view.

With the possibility that kerosene availability in the future will be less as compared to today due to the reduction in fossil fuels or increasing global warming or geopolitical unstable situation,

the LNG & Biofuel powered MF-BWB aircraft of AHEAD is a promising concept which can make aviation sustainable and affordable. The figure below shows the technology developed with AHEAD and its advantages and application.

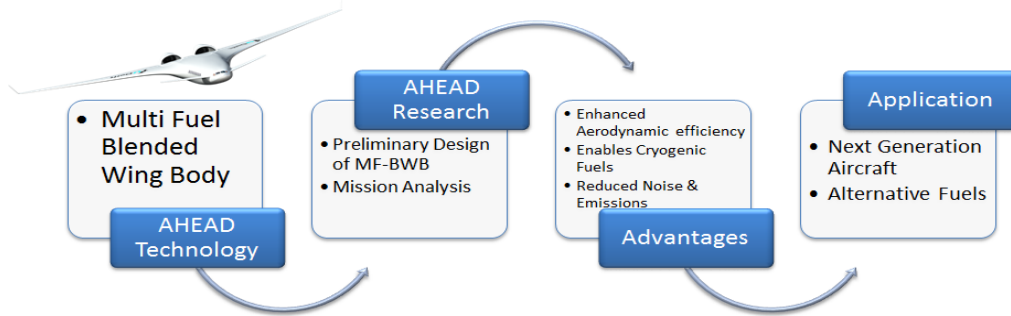


Figure 3.2: Research efforts performed on MF-BWB aircraft in the AHEAD project

### 3.2 The Hybrid Engine

Conventional engine architecture has reached a plateau and cannot be further improved. Moreover the increase in NOx with increasing efficiency is another challenge for the engine manufacturers. The present project provides a new insight into the solution of such problem, namely by using two combustion chambers. The effect of the AHEAD technologies on the entire engine value chain is depicted in Fig. 3.2. It can be seen that the AHEAD project has significant influence on the major components of the value chain.

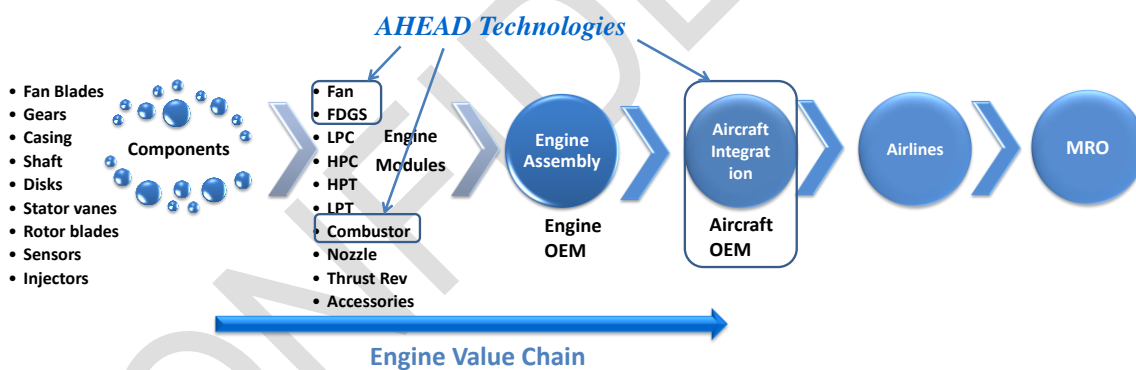


Figure 3.2: AHEAD Engine Technologies and the engine value chain

Since the architecture of the hybrid engine is quite different when compared to the conventional turbofan engines, the sizing and weight estimation of the engine is not trivial. In the AHEAD project initial investigations were made on the sizing of the two versions of the Hybrid engine, one based on the Geared Turbo Fan (GTF) architecture and the other on Contra-Rotating Turbo Fan (CRTF). At present there are no engines which have a BPR as the hybrid engine.

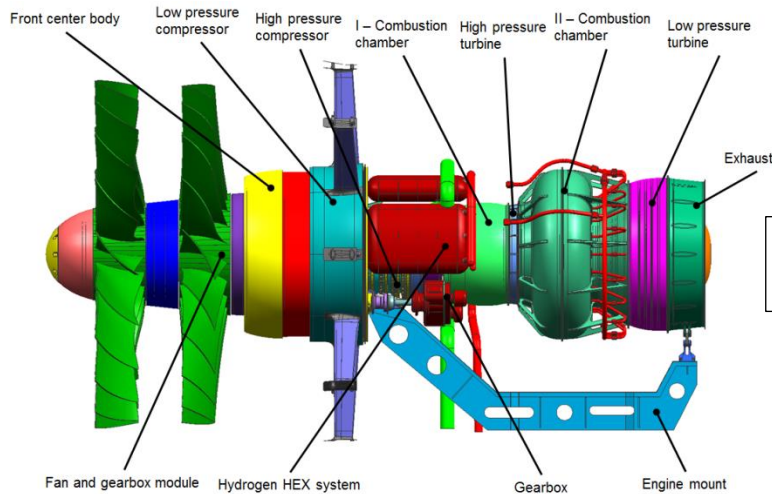


Figure 3.3: The AHEAD hybrid engine lay-out

### 3.3 CRF design

One of the main problems with BLI is the high amount of distortions encountered by the engine at the fan inlet. In the *AHEAD* project, we come-up with a novel idea to overcome this problem by using CRF instead of a single stage fan. The technology for CRF fan engines is not as mature as the technology for single fan engines. Therefore the project should in the short term decide on the fan configuration. This will also have an impact on the aircraft design in case buried engines are used. From the work carried out by the partners we know that the surge margin of a CRF could be increased by a well selected load balance between both rotors, due to lower aerodynamic loading and solidity of CRF. However this should be investigated further.

### 3.4 Cryogenic Heat exchanger

One of the novelties of the hybrid engine is the usage of the cryogenic fuel as a heat sink to increase the thermodynamic efficiency of the engine by using the cold fuel to cool the bleed air used for cooling the high pressure turbine (HPT) blades. This decreases the amount of air that is required for cooling the HPT blades and vanes. A preliminary design of a heat exchanger to heat the LH2 or LNG and to create cooling bleed air for the turbine vanes was carried out. The design needs to be finalized and a demonstrator needs to be built based on the heating/cooling requirements and desired flow mass of the LH2 and LNG fuel. This should be tested in a laboratory environment.

### 3.5 First combustion chamber

A new swirl stabilized premixed flame with axial air injection system was designed and demonstrated within the *AHEAD* project. Using this novel design, the combustion of LH2 (and LNG) was proven to be safe and without flashback. The technology and its enables and advantages are described in the Fig. 3.4 below. The application of this burner design can be extended to terrestrial applications like in industrial gas turbines used in the IGCC (integrated gasification and combine cycle) power plants. This design will also enable hydrogen to be used in other territorial applications.

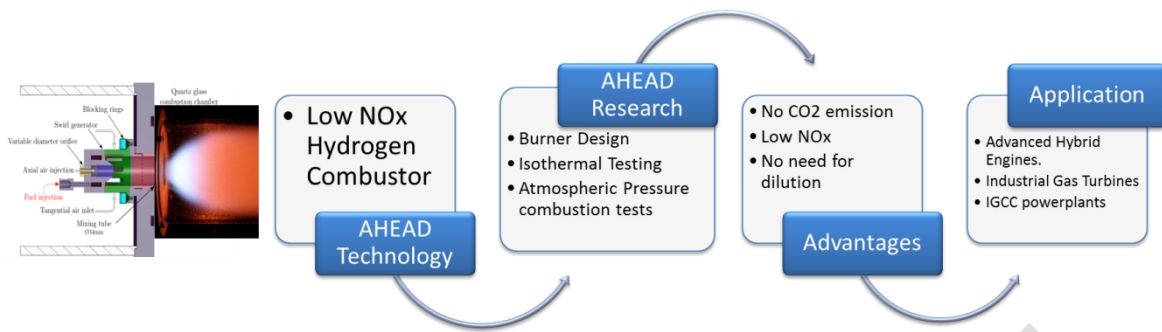


Figure 3.4: AHEAD research on the H2 combustion chamber

### 3.6 Flameless combustion chamber

The AHEAD showed the feasibility of flameless combustion as a secondary combustor within the Hybrid Engine architecture due to the high inlet temperatures and operating environment. For the first time a configuration was designed which could exploit the novel flameless combustion technology to its fullest. This design has the potential to be used in terrestrial gas turbines as well. By using the flameless combustion chamber as an inter-turbine burner, it is possible to reduce the NOx emission of future gas turbines substantially.

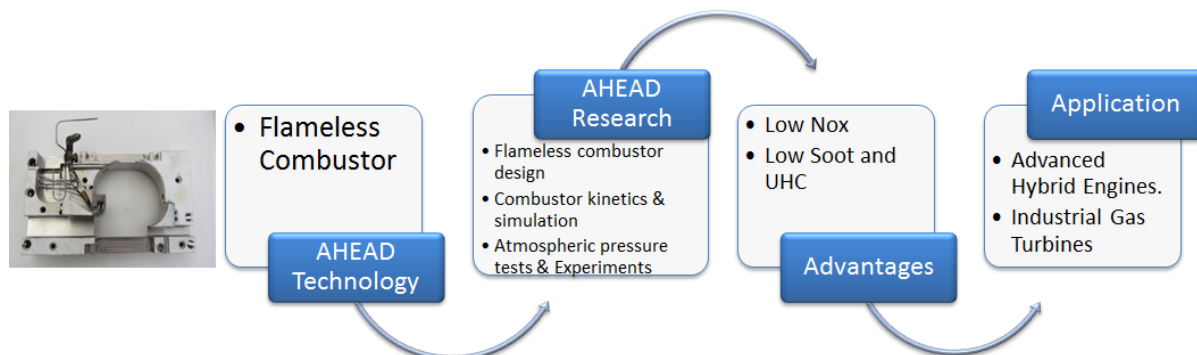


Figure 3.5: The AHEAD research on the flameless combustor

### 3.7 Climate Modelling

The AHEAD project was one of the few projects where the effect of aircraft on the climate was taken within the design phase. The results so far proved that this indeed was a prudent choice. This enabled the change the trajectory of the aircraft mission and helped in making sound choices regarding the future fuel for aviation. The AHEAD project also proved that climate can be used as a metric to make useful design trade-offs. The work carried out within the AHEAD project enabled to quantify the effect of soot particles on the contrail formation and clarified the effect of soot on the overall global warming.

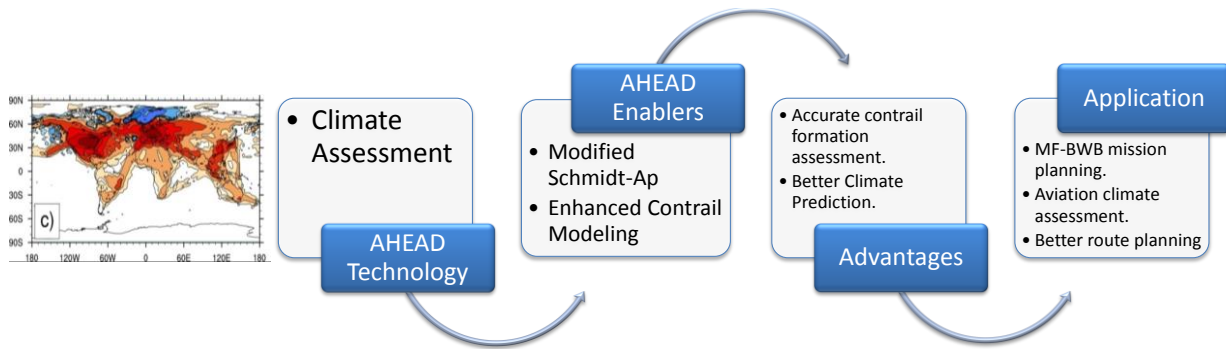


Figure 3.6: AHEAD climate assessment research

### 3.8 Impact on Cost

A detailed cost-benefit analysis was carried out within the AHEAD project to evaluate the financial viability of the aircraft. The B-777 was assumed to be the baseline aircraft. The table below summarizes the difference in cost between B-777 and MF-BWB aircraft. It can be seen that in the case of high CO<sub>2</sub> tax (20 Euros / tonne), the operating cost of MF-BWB aircraft with LNG & biofuel would be 26% less as compared to B777. In case if the CO<sub>2</sub> tax is low (5 Euros/tonne), the MF-BWB with LNG & biofuel would be 25% less when compared to B777. This is an enormous reduction in the operating cost which makes the case for LNG usage in aviation very strong.

	CO2 low	Co2 high
B777	€ 175,932	€ 182,654
MF BWB LNG	€ 131,662	€ 134,890
Difference	€ 44,270	€ 47,764
CO2 saving	174.7ton	174.7 ton
CO2 saving in %	52%	52%

### Address of project public website and contact details

The Address of project public website <http://www.ahead-euproject.eu>

Beneficiary No	Organisation	First name	Last name	Email address
1	TU Delft	Arvind	Gangoli Rao	A.GangoliRao@tudelft.nl
1	TU Delft	Jos	van Buijtenen	n/a
1	TU Delft	Feija	Yin	F.Yin@tudelft.nl
1	TU Delft	Jan	Vriend	n/a
1	TU Delft	C.	Huo	n/a
1	TU Delft	Abhishek	Bhat	A.Bhat@tudelft.nl
1	TU Delft	Dipanjay	Dewanji	n/a
1	TU Delft	Mark	Voskuijl	M.Voskuijl@tudelft.nl
1	TU Delft	Theresia	Twickler	n/a
1	TU Delft	Dunja	Swierstra	D.A.M.Swierstra@tudelft.nl
1	TU Delft	Helma	van den Bos	Helma.vandenBos@tudelft.nl
1	TU Delft	Ernst	Harting	E.J.Harting@tudelft.nl
1	TU Delft	Alwin	Wink	A.D.Wink@tudelft.nl
2	WSK	Robert	Haligowski	Robert.Haligowski@wskrz.com
2	WSK	Andrzej	Cwik	Andrzej.Cwik@wskrz.com
3	TU Berlin	Oliver	Paschereit	oliver.paschereit@tu-berlin.de
3	TU Berlin	Sebastian	Goeke	n/a
3	TU Berlin	Thoralf	Reichel	thoralf.reichel@tu-berlin.de
4	DLR	Volker	Grewe	Volker.Grewe@dlr.de
4	DLR	Klaus	Gierens	Klaus.Gierens@dlr.de
4	DLR	Ulrike	Burkhardt	Ulrike.Burkhardt@dlr.de
4	DLR	Lisa	Bock	Lisa.Bock@dlr.de
5	Technion	Yeshayahou	Levy	levyy@aerodyne.technion.ac.il
5	Technion	Akiva	Sharma	n/a
6	ADC	Ad	de Graaff	adgraaff@hetnet.nl